The synthesis and characterization of sodium polysulfides for Na-S battery application

Qiaoyi Zhang

Thesis submitted to the faculty of the

Virginia Polytechnic Institute and State University

In partial fulfillment of the requirements for the degree of

Master of Science

In

Chemical Engineering

Zheng Li Co-chair

Hongliang Xin, Co-chair

William Ducker

May, 1st, 2019

Blacksburg, VA

Keywords: Sodium polysulfides, Synthesis, Na-S battery

The synthesis and characterization of sodium polysulfides for Na-S battery application

Qiaoyi Zhang

ABSTRACT

The limited understanding of the electrochemical mechanism of Na-S battery systems is a barrier to further improve the performance of the Na-S energy storage. The characterization of sodium polysulfides in the Na-S battery systems can offer insightful information to understand the electrochemical reaction mechanism of the Na-S batteries and overcome the "inert" nature of short-chain polysulfides (Na_2S_n, $1<n<4$) during charge and discharge of the batteries. Up to now, there are limited studies on the sodium polysulfides compound in the Na-S batteries. Meanwhile, although many synthesis methods for sodium polysulfides have been reported, many related studies offer unclear and misleading parameters.

This work examines several reported synthesis methods for sodium polysulfide. The results show that the sodium polysulfides cannot be obtained by the reaction of Na_2S and S using anhydrous ethanol as the reaction media. In "dry" synthesis method, the pressure will influence the components in the product, and only Na_2S_4 can be synthesized at atmospheric pressure. This study also revises the synthesis method for Na_2S_2 and Na_2S_5, and detailed synthesis parameters are presented.

The properties of sodium polysulfides in tetraethylene glycol dimethyl ether TEGDME were studied in this thesis. The solubility of Na_2S_n in TEGDME increases with increasing sulfur in sodium polysulfide. The corresponding solution gets to longer-wavelength color and contains more long-chain polysulfides anions (S_n^{2-}, $4<n<8$).

The synthesis and characterization of sodium polysulfides for Na-S battery application

Qiaoyi Zhang

GENERAL AUDIENCE ABSTRACT

In recent decades, our society became more and more power-demanding, sodium-sulfur (Na-S) energy storage systems attracted researchers' attention due to their low cost and good performance. However, the limited understanding of the electrochemical mechanism of Na-S battery systems is a barrier to further improve the performance of the Na-S batteries. The characterization of sodium polysulfides in the Na-S battery systems can offer insightful information to understand the working mechanism of the Na-S batteries during charge and discharge of the batteries.

Up to now, there are limited studies on the sodium polysulfides compound in the Na-S batteries. Meanwhile, although many synthesis methods for sodium polysulfides have been reported, many related studies offer unclear and misleading parameters. This work examines several reported synthesis methods for sodium polysulfide and offers complete processes with clear parameters for the synthesis of sodium polysulfide. Meanwhile, the sodium polysulfides solution in tetraethylene glycol dimethyl ether (TEGDME), an electrolyte solvent that was widely used in Na-S batteries, were analyzed to study the properties of sodium polysulfides in the Na-S battery system.

Acknowledgment

Foremost, I would like to express my sincere gratitude to my advisors, Dr. Zheng Li and Dr. Hongliang Xin, for their continuous support of my M.S. Study and research, for their patience, motivation, enthusiasm, and immense knowledge. Their guidance helped me in all the time of research and writing of this thesis.

Besides my advisors, I would like to thank the rest of my thesis committee: Dr. William Ducker, for his encouragement, insightful comments, and hard questions.

My sincere thanks also goes to, Dr.Weinan Leng, Dr, Stephen Martin, Ethan Smith, Dr. Wenhui Li. Also, thanks for the help from Dr.Sanpei Zhang, Panni Zheng, Dayang Ge, and all my labmates.

Last but not the least, I would like to thank my parents for supporting me spiritually throughout my life.

Table of Contents

List of Figures

Chapter 1: Introduction

1.1 Motivation

In recent decades, our society became more and more power-demanding, efficient mobile and stationary energy storage systems attracted researchers' attention. The Na-S energy storage systems became promising candidates in energy storage application due to their high power and energy density and lower cost of the electrode materials. Since the1960s, the Ford Motor Company first released their research result about Na-S energy storage systems, after that, there are many related successful technologies reported, furthermore, the theory of traditional high-temperature sodium-sulfur energy storage technology has already been commercially demonstrated [1-3]. In 2006, Korean researchers reported that the room-temperature Na-S battery technology is able to further improve the performance and safety of the Na-S energy storage system [4].

Although, there were many studies about Na-S energy storage systems reported, the limited understanding of the electrochemical mechanism of Na-S battery systems provide a barrier to further improving the performance of the Na-S energy storage. By applying sodium polysulfides in the Na-S battery systems, researchers will have a deeper understanding of the electrochemical mechanism in the systems, and more information can be obtained to overcome the "inert" nature of short-chain polysulfides (Na_2S_n, $1<n<4$) during charge and discharge of the batteries. Up to now, there are limited studies that apply the sodium polysulfides compound in the Na-S batteries.

Meanwhile, currently reported synthesis methods are also needed to be revised. Although many synthesis methods for sodium polysulfides have been reported, most studies did not offer clear

processing parameters, furthermore, some related studies even reported misleading processing parameters.

1.2 Research Objectives

The main objective of this research is to have a deeper insight into the working mechanism of sodium-sulfur batteries and offer more valuable information to further improve the performance of Na-S energy storage systems.

The first goal of this research is to establish a complete synthesis process for sodium polysulfide which cannot be commercially obtained based on the sodium polysulfides synthesis method reported. And this study aimed to offer clear and detailed synthesis procedure and parameters for each sodium polysulfide. The second goal of this research is to analyze the electrochemical reactions happening in the electrolytes in Na-S energy storage system using the synthesized sodium polysulfide product.

Chapter 2 Background and Literature Review

2.1 Sodium- Sulfur Battery

In recent decades, our society became more and more power-demanding, efficient mobile and stationary energy storage systems attracted researchers' attention [5-8]. As shown in **Fig.1**, among various existing and reported energy storage systems, sulfur-containing batteries, such as lithium-sulfur batteries, and sodium sulfur batteries, are particularly attractive due to the high power and energy density and low cost of sulfur [9-13].

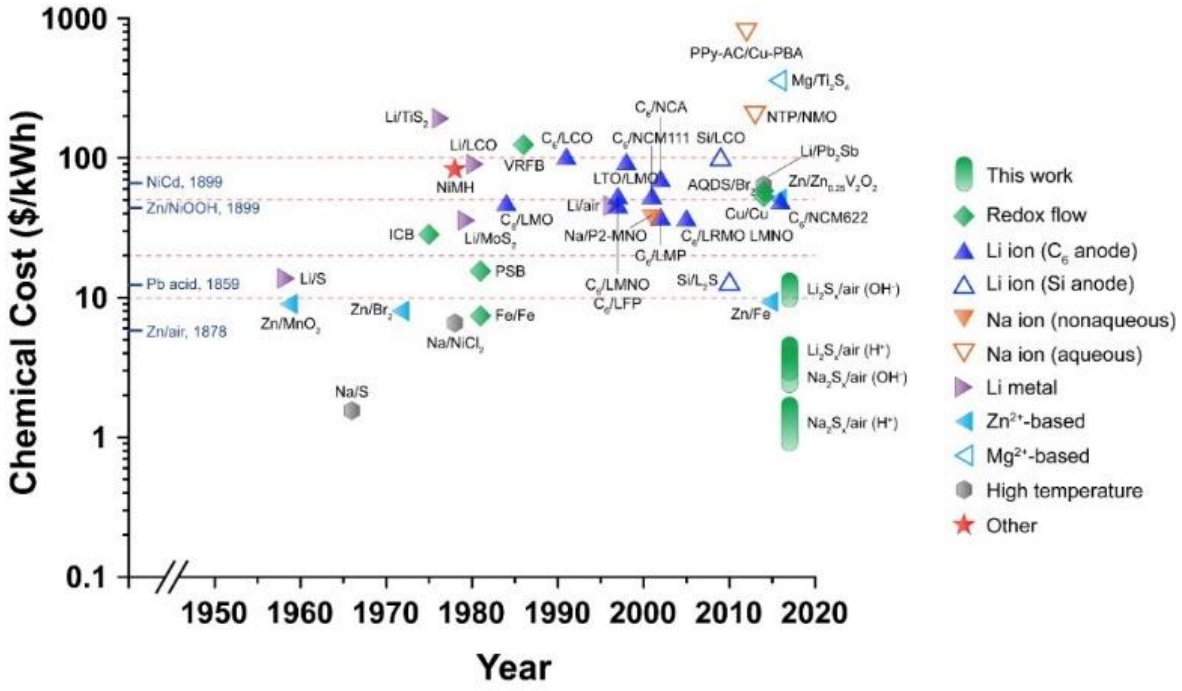

(a)

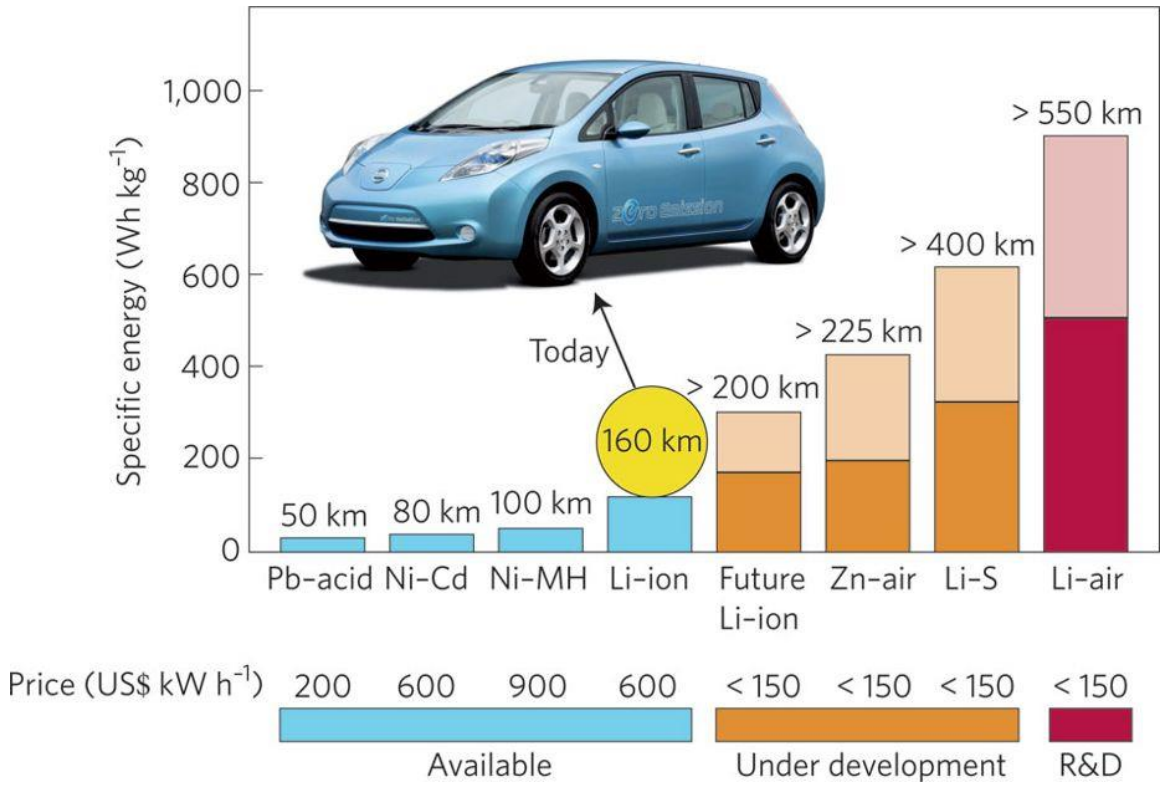

(b)

Figure 1 Comparison of the cost and specific energy of metal-sulfur batteries and other rechargeable batteries. (a. The chemical cost of reported energy storage systems. Reprinted with permission from [9] b. Specific energies for some rechargeable batteries. Reprinted with permission from [10])

Although the low cost of sulfur decreased the total cost batteries and increased the specific energy of Li-based batteries, Li-S batteries still can hardly meet the need of relatively large-scale stationary battery due to the limited natural abundance and the high price of lithium [14]. Hence, because of the much larger abundance and lower price of Na, and its suitable redox potential,

$E^{0}_{(Na^{+}/Na)} = 2.71V$, sodium sulfur batteries were highlighted as a promising candidate for energy storage applications since the 1980s.

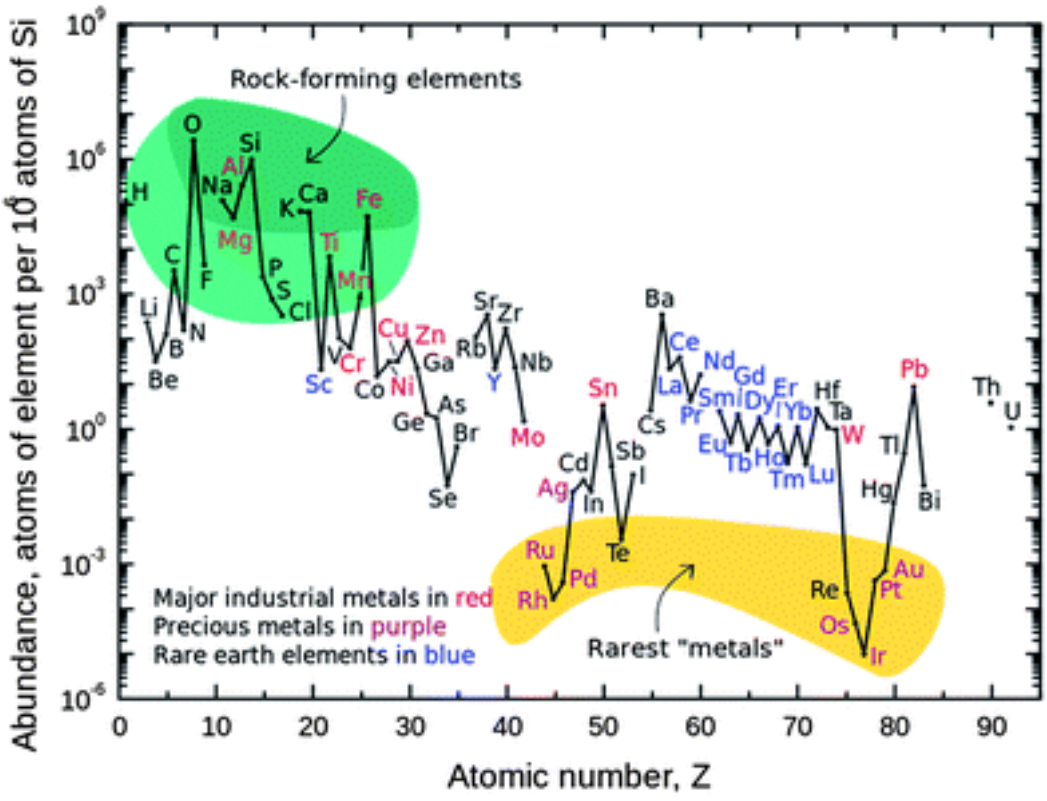

Figure 2 . Natural elemental abundances in the earth's crust [15]

In Na-S batteries, sodium acts as the anode, sulfur works as the cathode, and a sodium-ion-conductive electrolyte and a separator used for Na+ ion transition. This kind of energy system works based on the reversible electrochemical reaction of Na-S system [16]. Up to now, there are many successful Na-S battery technologies reported, the theory of traditional high-temperature sodium-sulfur energy storage technology has already been commercially demonstrated [1-3].

In the 1960s, scientists at the Ford Motor Company first reported the details of the Na-S energy storage systems, a tubular structure was used in the reported system because this design minimizes the influence of the volume change during cycling and the sealing area [1, 17]. The composition of the tubular molten Na-S batteries can be explained by **Fig.3**.

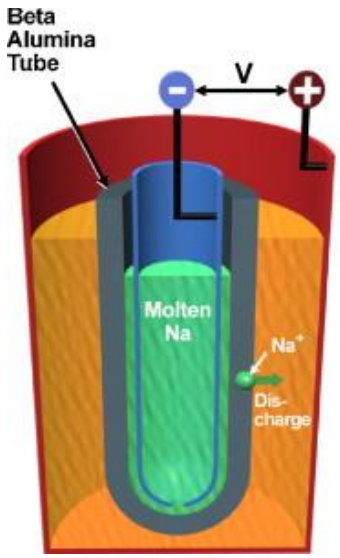

Figure 3 . Schematic of the tubular Na-S cell. Reprinted with permission from [12]

The working mechanism of high-temperature Na-S battery cell during charge and discharge can be explained by **Fig.4**. While discharge, the anode is oxidized from metal Na to Na^+ ions as reaction described in Eq. (1), then transfers through the beta-Al_2O_3 ceramic electrolyte membrane and combines with reduced polysulfide anions [18], Sn^{2-}, to generate sodium polysulfide Na_2S_n in the cathode (the cathode reaction was shown in Eq. (2)).

Anode reaction:

$$2Na = 2Na^{+} + 2e^{-} \quad (1)$$

Cathode reaction:

$$nS + 2e^{-} = S_n^{2-} \quad (2)$$

Overall reaction:

$$2Na + nS = Na_2S_n \quad (3)$$

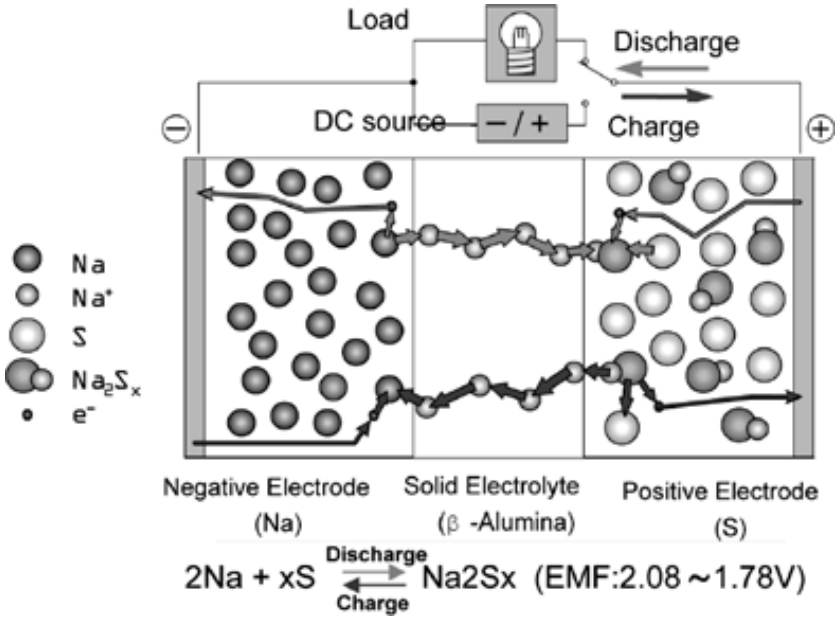

Figure 4 High-temperature Na-S battery cell principle of operation. Reprinted with permission from [16]

The operating temperature of high-temperature Na-S batteries is about 270 to 350 ℃, thus, the electrodes in Na/S batteries are molten sulfur (melting point at 113.2℃ at 1 atm) as the cathode and molten sodium (melting point at 97.8℃ at 1 atm) as the anode. The sodium-ion conductive beta-alumina ceramics acts as both electrolyte and separator in molten Na-S batteries. During discharge, electrons that are stripped off from the anode move through the external circuit, combined with the sulfur in the cathode, then generate polysulfides, then Na+ can transport across the solid ceramics to the cathode to balance the electron charge. Electrochemical reactions are reversed during charge. The OCV profile versus the state-of-charge that suggested by Oshima et al.[16] was illustrated in **Fig.5**, according to this hypothesis, at high state-of-charge, S and initially formed Na_2S_5 co-existing phase in the cathode shows an OCV of 2.075V. Then, reduction of sulfur and polysulfide occurs from 2.075V to 1.74V, at 1.74V, sulfur and polysulfides convert to Na_2S_3, meanwhile a new phase forms. For deeper discharge, the cathode is further reduced to Na_2S_2, a solid discharge product.[3].

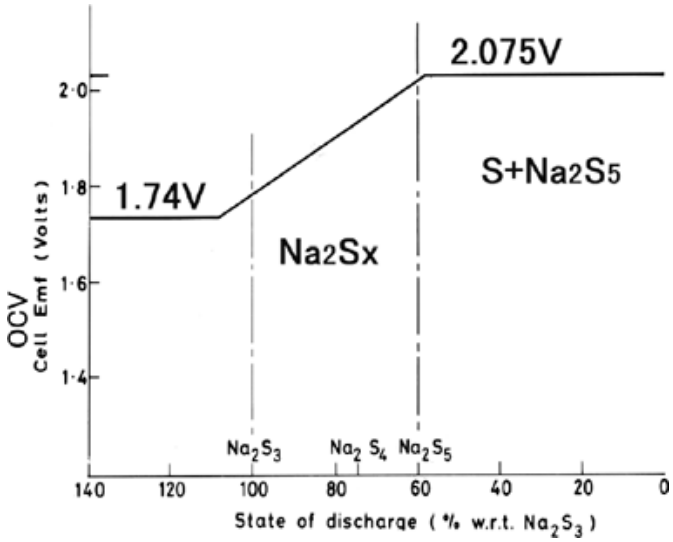

Figure 5 Representation of the voltage profile for High-temperature Na-S cell with phases present at each stage. Reprinted with permission from [16]

In the 1980s, NGK and Tokyo Electric Power Company successfully developed the Na-S battery technology, and NGK commenced commercial Na-S energy storage systems in Japan. Despite the high efficiency of Na/S systems in general (normally around 89%), the high operating temperature and the corrosive sodium polysulfides in systems might cause safety issues, which limited them for wide range applications. Meanwhile, an independent heater must be used to keep the operating temperature to guarantee the process of the whole Na-S battery system. To this end, low-temperature Na-S batteries might offer a more promising way for low-cost, high-capacity energy storage systems [19-23], otherwise, the low operation temperature might offer a safer way for energy storage, although this technology should be further revised to improve the performance of the battery and to mitigate some safety concerns when applying in the commercial-scale products.

Low-temperature Na-S batteries can operate at room temperature or just below 100 ℃. When Korean researcher Hyo-Jun Ahn and his group first reported room-temperature Na-S batteries [4], they used $NaCF_3SO_3$ PVDF gel polymer electrolyte to conduct sodium ion. Conventional separators, such as glass fibers, and sodium salt solutions in organic electrolytes can be applied in low-temperature Na-S batteries directly. As shown in **Fig.6**, the room-temperature Na-S cell can be assembled similarly with room-temperature Li-S batteries, with sulfur or sulfur-containing cathode and sodium metal anode. A sodium salt (such as $NaClO_4$ [14, 24, 25], $NaCF_3SO_3$ [26-28], $NaPF_6$ [29-31], et.al) solution in an organic solvent (such as PC/EC(v:v=1:1) [22], TEGDME [32], EC/DEC(v:v=1:1) [30], etc.) works as electrolyte for the transport of sodium ion. And sometimes,

there will be an interlayer between the cathode and the separator as a polysulfide inhibitor to avoid the negative influence of shuttle effect. Similarly, with high-temperature Na-S batteries, while discharging, sodium anode oxidizes to Na^+ and produce electrons, the electrons will transfer to the cathode to form S_n^- through the external circuit, meanwhile, the sodium ions pass through the electrolyte and the separator and combine with S_n^- produced by the reduction of sulfur in the cathode to form sodium polysulfides.

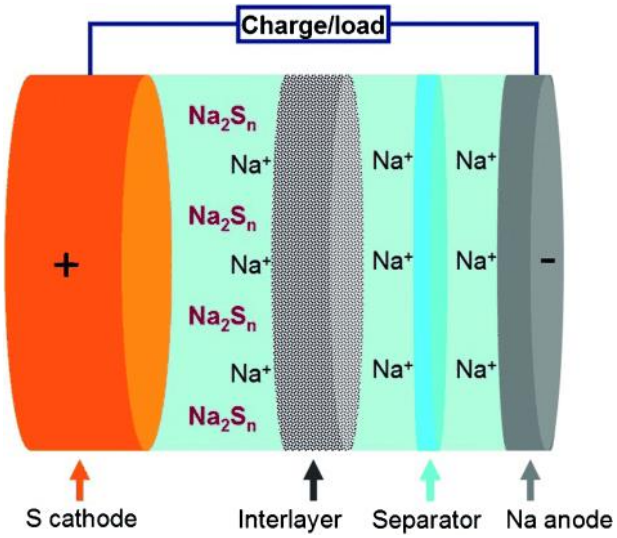

Figure 6 Schematic configuration of a room-temperature Na–S battery with an interlayer between the cathode and the separator. Reprinted with permission from [33]

According to Yu et al.'s research, the discharge process of room-temperature can be divided into four steps, shown in **Fig.7**. In the region I, there is a plateau at 2.2V, corresponding to the following reaction.

$$S_8+2Na^++2e^- \rightarrow Na_2S_8 \quad (4)$$

And there is an inclined region after region I in the voltage range from around 2.20 to 1.65V, and there is a liquid-liquid reaction happening in this state, namely, the dissolved Na_2S_8 is being reduced to Na_2S_4 by the following mechanism.

$$3Na_2S_8+2Na^++2e^- \rightarrow 4Na_2S_6 \quad (5)$$

$$6Na_2S_6+2Na^++2e^- \rightarrow 5Na_2S_5 \quad (6)$$

$$4Na_2S_8+2Na^++2e^- \rightarrow 5Na_2S_4 \quad (7)$$

In the third state, there is a low-voltage plateau at about 1.65V, in this region, insoluble Na_2S_3 and Na_2S_2 are formed.

$$3Na_2S_4+2Na^++2e^- \rightarrow 4Na_2S_3 \quad (8)$$

$$Na_2S_4+2Na^++2e^- \rightarrow 2Na_2S_2 \quad (9)$$

$$2\ Na_2S_3+2Na^++2e^- \rightarrow 3Na_2S_2 \quad (10)$$

Region IV is another inclined region in the range of 1.65 to about 1.20V occurs in the last state, the polysulfides can further be reduced to insoluble Na_2S_2 and Na_2S.

$$2\ Na_2S_2+2Na^++2e^- \rightarrow 2Na_2S \quad (11)$$

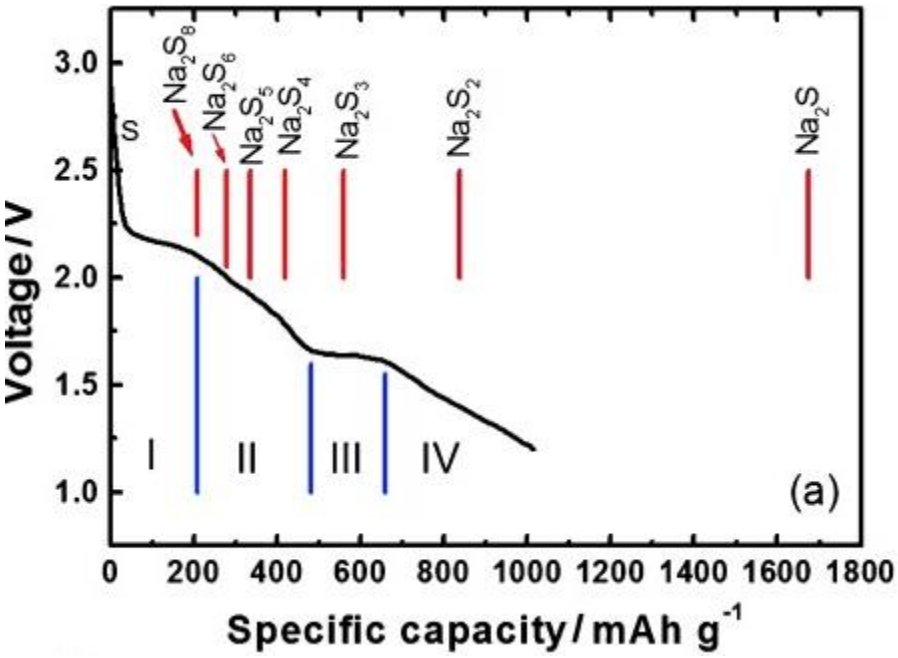

Figure 7 Theoretical versus practical discharge capacities. Reprinted with permission from [33]

Theoretically, low-temperature sodium-sulfur batteries have higher capacity than high-temperature cells due to the temperature difference. However, most reports fail to realize even half of the theoretical gravimetric capacity of the sulfur cathode (1673 mAh/g) [3, 14, 27, 32, 34, 35]. Although theoretical data of the electrochemical reaction can be illustrated as above-mentioned electrochemical equations, the detailed mechanism at room temperature still needs deeper studies to further improve the room-temperature Na-S battery technology.

2.2 Sodium- sulfur System

The Na-S system has been widely investigated to obtain a deep understanding of the nature of polysulfides. The study of Na-S system also offered information for industry, for example, the theory of Na-S system can offer clues to improve the performance of Na-S high energy-density storage system [16, 36].

In 1914, K. Friedrich et al. [37] first published the sodium-sulfur phase diagram. In their research, he postulated the existence of several tetrasodium polysulfides (Na_4S_n, n= 3, 5, 7, 9, etc.). After that Rule and Thomas offered a further investigation and claimed that only the disodium polysulfides (Na_2S_n, n=1, 2, 3, 4, etc.) can be established as compounds [38, 39]. And Pearson et al.[40] confirmed their results and revised the Na-S diagram (**Fig.8**).

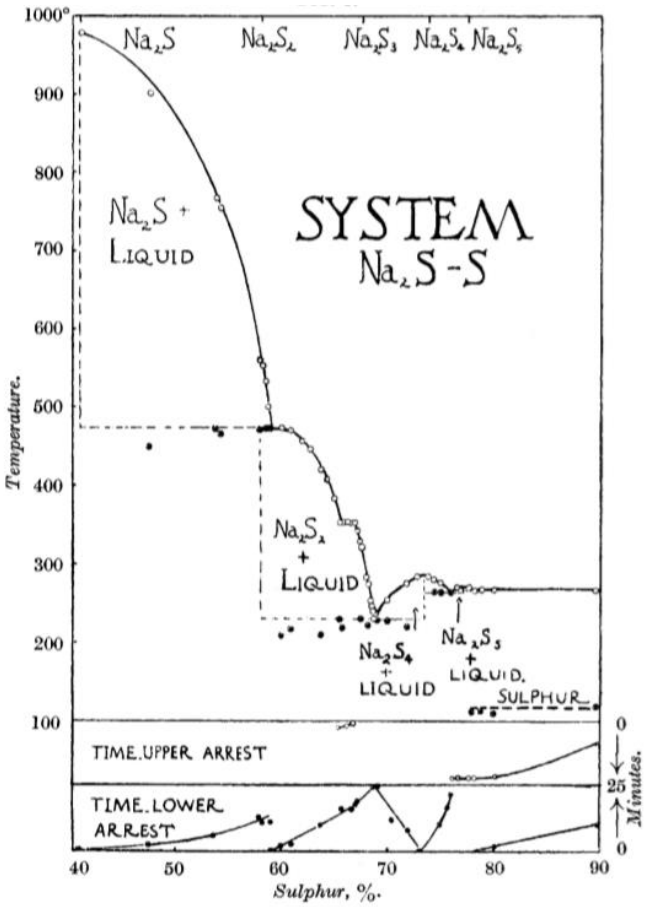

Figure 8 The assessed Na-S phase diagram. Reprinted with permission from [40]

40 years later, the partial pressure of sulfur was calculated from the sodium activities via Gibbs-Duhem equation, and all these results were used for analysis to add optimized iso-P_{S2} curves in the Na-S phase diagram [41]. After taking the partial pressure of sulfur into consideration, an assessed Na-S phase diagram with the isobaric curve of the partial pressure of sulfur can be illustrated as **Fig.9**, which can be used as a reference for Na-S battery design and the synthesis of sodium polysulfides.

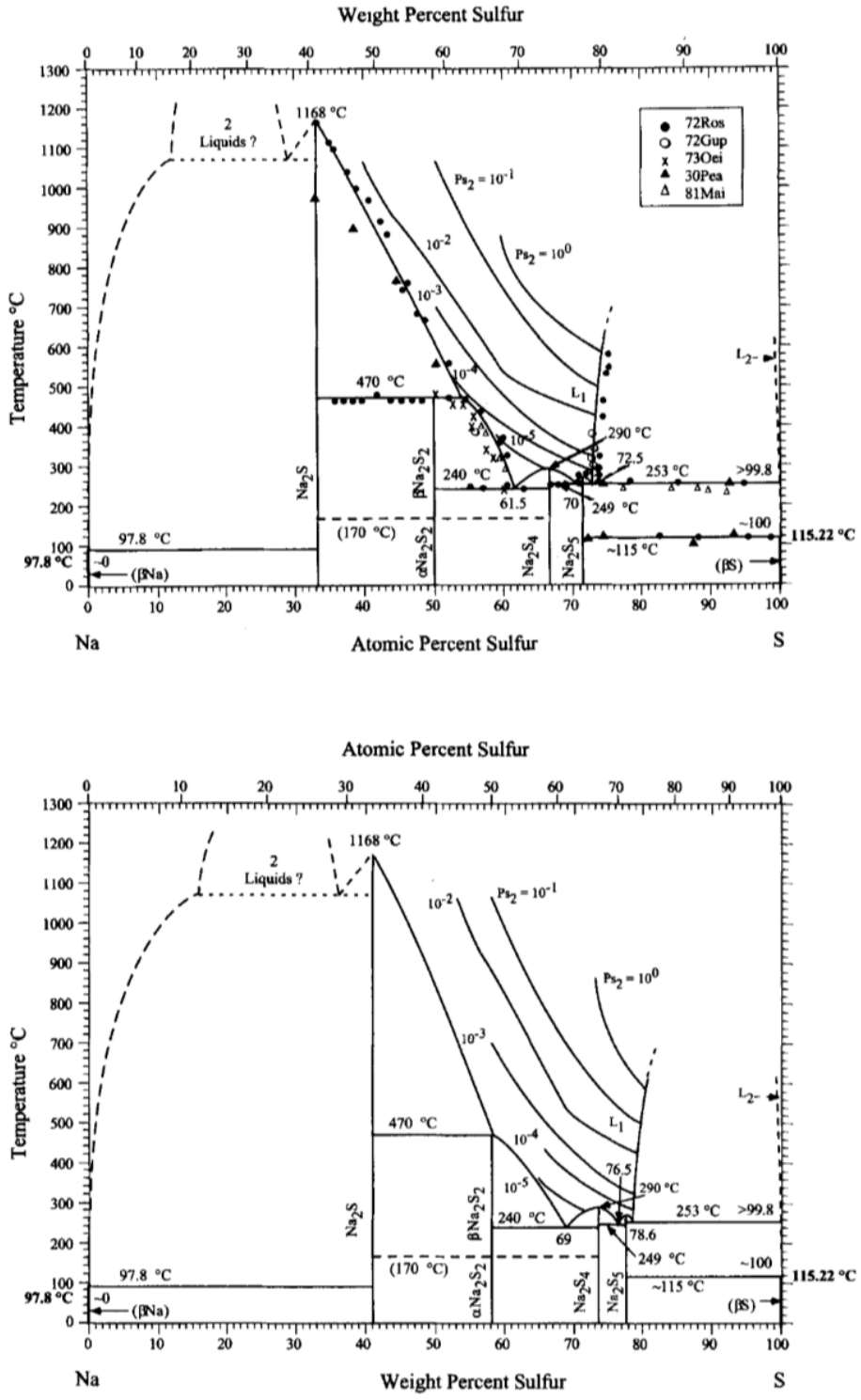

Figure 9 Assessed Na-S phase diagram including the isobar of the pressure of S_2. Reprinted with permission from [42]

2.3 Current Synthesis Method for Sodium Polysulfides

As illustrated above, the study of the sodium-sulfur system can offer valuable information for Na-S density storage system. The sodium polysulfides can also be applied in the Na-S batteries and study the working mechanism of Na-S batteries. For example, to screen the impact from the reaction of S_8 to long-chain Sn^{2-}, Yu et al. dissolved Na_2S and S stoichiometrically (Na_2S:S=1:5) in TEGDME, and used this solution as the intermediate product, Na_2S_6, as the starting cathode to study the lower-voltage-plateau region of Na-S batteries [14]. Kim et al. [25] used the same method to prepare intermediate product sodium polysulfides to study the Na-S batteries. In 2015, Yu et al.[43] prepared a Na_2S cathode by spreading the multi-walled carbon nanotube (MWCNT)-wrapped Na_2S particles onto MWCNT fabrics to study the Na-S batteries and try to overcome the "inert" nature of Na_2S. However, there are limited studies using sodium polysulfides compounds as the intermediate in the cathodes, Na_2S_n compounds will help to have a better understanding of Na-S battery. Up to now, there are several methods reported for the synthesis of sodium polysulfides.

2.3.1 Na_2S – Sodium Sulfide

Anhydrous state Na_2S can be prepared by element sodium and sulfur in protecting media [44, 45], drying $Na_2S{\cdot}9H_2O$ or the reduction of Na_2SO_3 and Na_2SO_4 by S, C or H_2. When synthesizing elements sodium and sulfur, the reaction is performed in anhydrous liquid ammonia according to Eq.12. A N_2 or CO_2 cooling bath can be used to keep the temperature of the liquid ammonia during the reaction. After the reaction is completed, the NH_3 media will be evaporated [46].

$$2\ Na + S \rightarrow Na_2S \quad (12)$$

Anhydrous Na_2S can also be obtained by drying pure $Na_2S \bullet 9\ H_2O$. Pure $Na_2S \bullet 9\ H_2O$ should be stored over superabsorbent agents, such as concentrated H_2SO_4 or H_3PO_4 in a vacuum desiccator for about 14 days. The operating temperature should be around 15 °C in the initial phase and can be raised slightly to about 35 °C [47]. The reaction equation can be illustrated as Eq.13.

$$Na_2S \bullet 9\ H_2O \xrightarrow{\text{Concentrated } H_2SO_4 \text{ or } H_3PO_4 \text{(vacuum)}} Na_2S + 9\ H_2O \quad (13)$$

Commercially, anhydrous Na_2S can also be prepared by the reduction reaction of Na_2SO_4 using C, CO or H_2. However, this method is not able to produce a sufficiently pure product [48]. Anhydrous Na-S is a white hygroscopic crystalline compound, it will change color in moist air and has a melting point of 1180 ± 10 °C (under vacuum).

2.3.2 Na_2S_2 – Sodium Disulfide

There are three synthetic methods that were reported to prepare sodium disulfide. Firstly, it can be synthesized by elemental sodium and sulfur in the ammonia media by the same method as Na_2S [46]. Sod odium disulfide can also be obtained by the reaction of sodium tetrasulfide with sodium in the media. A stoichiometric amount of metal sodium was added into the prepared Na_2S_4 ethanol solution under N_2, according to Klemm et al.'s report, the precipitate of Na_2S_2 can be obtained [38].

$$Na_2S_4 + 2Na \rightarrow 2Na_2S_2 \quad (14)$$

Besides, Na_2S_2 can be obtained by the reaction of Na_2S and S. Appropriate stoichiometric amount of Na_2S and S are heated at 500 °C under vacuum to obtain beta-Na_2S_2 according to the following reaction equation.

$$Na_2S + S \xrightarrow{500\ ^\circ C\ (vacuum)} Na_2S_2 \quad (15)$$

Na_2S_2 is a light yellow, microcrystalline, very hygroscopic powder. The melting point is approximately 490 °C.

2.3.3 Na_2S_3 – Sodium Trisulfide

Na_2S_3 can be obtained by the reaction of the elemental sodium and sulfur in liquid ammonia media or from the melt Na_2S_2 and Na_2S_4 stoichiometrically, but the XRD of Na_2S_3 shows that the product is a mixture of Na_2S_2 and Na_2S_4[49].

2.3.4 Na_2S_4 – Sodium Tetrasulfide

Similarly, Na_2S_4 can be obtained by elemental sodium and sulfur in ammonia media or by heating Na_2S and stoichiometric amount S under vacuum. It also can be obtained by the reaction between Na and sulfur according to the following reaction [50].

$$2NaHS + 3S \rightarrow Na_2S_4 + H_2S \quad (16)$$

2.3.5 Na_2S_5 – Sodium pentasulfide

Na_2S_5 has been successfully synthesized by the reaction of elemental sulfur and sodium. Na_2S_5 is orangish yellow powder, and very hygroscopic.

Although many synthesis methods for sodium polysulfides have been reported, most studies did not offer clear processing parameters, furthermore, some related studies even reported misleading

processing parameters. This study studied the operating conditions for sodium polysulfides synthesis and offered clear procedures and parameters for each sodium polysulfide synthesis.

2.4 Characterization of Sodium Polysulfides in Na-S battery

2.4.1 Powder X-ray diffraction

XRD is one of the most common characterization methods for powder sample, it can characterize the phase composition of the crystalline material and offer information about the crystalline structure of the material. XRD is widely used in the characterization of the discharge products in the cathode of Na-S battery system and the study of the crystalline structure of the sodium polysulfides. **Fig.10** shows Mali et al.[49]'s structure refinement study of sodium polysulfides basis the XRD patterns.

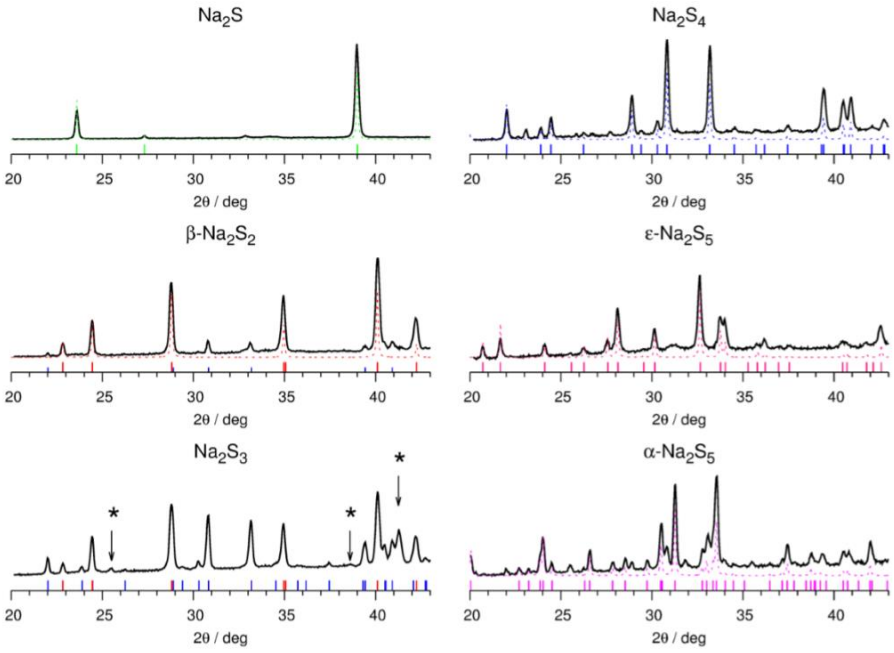

(a)

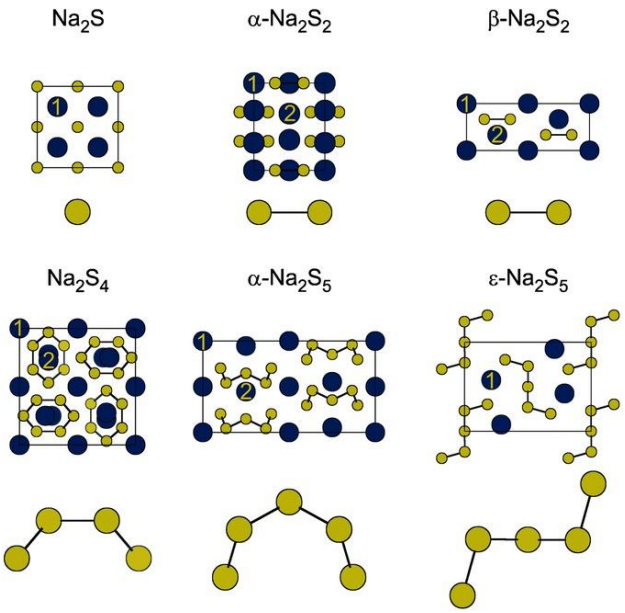

(b)

Figure 10 Structure refinement study of sodium polysulfides (a. XRD patterns of sodium polysulfides, b. Unit cells of crystalline sodium polysulfides. Reprinted with permission from [49]

2.4.2 Raman spectroscopy

Raman spectroscopy uses an analysis of scattered light to characterize the molecular vibration, which can provide a structural fingerprint and is commonly used to identify the species of molecules, cations, and ions. It is spectroscopic technique used to observe vibrational, rotational and other low-frequency modes in a system by Raman effect. The Raman effect is based on the interaction between the electron cloud of a sample and the external electric field of the monochromatic light, which can create an induced dipole moment within the molecule based on its polarizability. Raman spectroscopy is widely used as an ex-situ method to characterize the composites of electrodes and electrolytes [51-56], sometimes, combined with other

characterization techniques, such as XRD, FTIR, etc. Raman can be applied on both solid and liquid samples, and is nearly non-destructive for the testing sample, except laser or light-sensitive materials, otherwise, it can be quickly performed. Because of above merits, Raman spectroscopy is widely used in the study of polysulfide and metal-sulfur battery systems, Yeon et al.[51]applied in-situ Raman spectroscopy to theirs study about Li-S battery to investigate the reaction mechanism that limits the capacity, as shown in **Fig.11**, they found Li_2S cannot be found in the discharged cathode, the capacity of the battery might be limited by the diffusion-control reaction from insoluble Li_2S_2 to Li_2S.

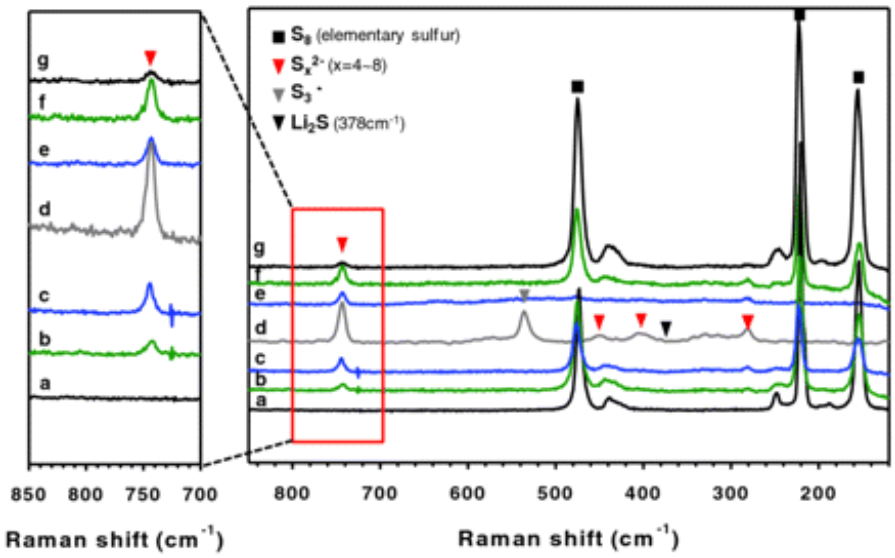

Figure 11 Raman spectra of sulfur cathodes obtained from seven representative points (a. Pristine cathode. b. Discharged to 2.28 V. c. Discharged to 2.1 V. d. Full discharge. e. Charged to 2.34 V. f. Charged to 2.4 V. g. Full charge.) Reprinted with permission from [51]

2.4.3 Fourier transform infrared spectroscopy (FTIR)

FTIR can identify molecular bond and structure of both solid and liquid. Contrast with Raman spectroscopy, in FTIR, energy of absorbed photon matches the difference in energy between the initial and final rovibronic states. The FTIR characterization mainly depends on the change in dipole moment. If a bond is strongly polarized, a small change in its length such as that occurs during a vibration, will have only a small additional effect on polarization. Due to the electrical characteristic of the vibration, the strong bands in infrared spectrum of one compound often corresponds to weak bands in the Raman spectrum. Hence, FTIR is complementary to Raman spectroscopy, it can be applied in the study of batteries combined with Raman spectroscopy.

Dillard et al. [57] studied the interactions between redox species in the Li-S batteries, they applied in-situ ATR-FTIR with attenuated total reflection to monitor both polysulfides and electrolyte during charging and discharging. **Fig.12** shows the schematic of the in-situ ATR-FTIR experiment in their study. Hence, FTIR is able to characterize the discharge product in electrode materials and the state of charge in Na-S batteries [58].

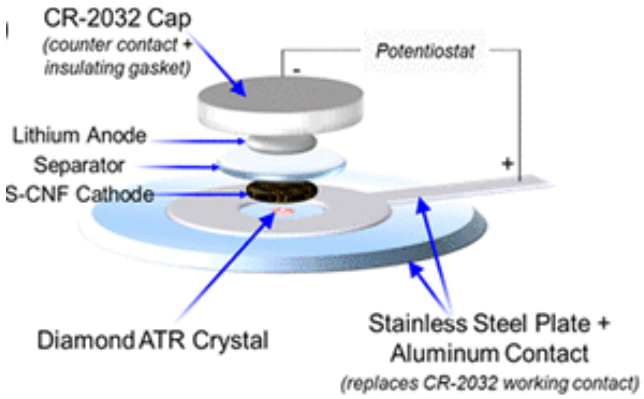

Figure 12 Schematic of the in situ infrared spectroelectrochemical experiment with a lithium-sulfur cell on the ATR crystal of the FT-IR spectrometer. Reprinted with permission from [57]. Copyright (2019) American Chemical Society.

2.4.4 Electron spin resonance (EPR) spectroscopy.

EPR spectroscopy is an efficient strategy to fully investigate the electrolyte composition, as previously reported in the literature. This technique can measure the diffusion of various materials, such as transition metal ions and organic free radicals [59, 60]. The direct EPR spectroscopy comparison of the electrolyte composition before and after cycles helps us investigate the crossover effect on the electrochemical performance. The EPR spectroscopy technique has been recently developed to probe the polysulfides species in the electrolyte [61, 62]. For example, Barchasz et al. reveal the $S_3^{\bullet-}$ radical in the electrolyte during the discharge and charge process, resulted from the disproportionation reaction (**Fig.13**) [63]. The special $S_3^{\bullet-}$ radical was produced during the first step and then consumed along with the electrochemical process. In Vijayakumar et al.'s[64] investigation about the stability of PS electrolyte and the influence of solvents on the electrochemical reaction of polysulfide in the for Li-S batteries, they probed the intermediates to have a further insight of the electrochemical step of lithium polysulfides dissolved in the electrolyte by EPR.

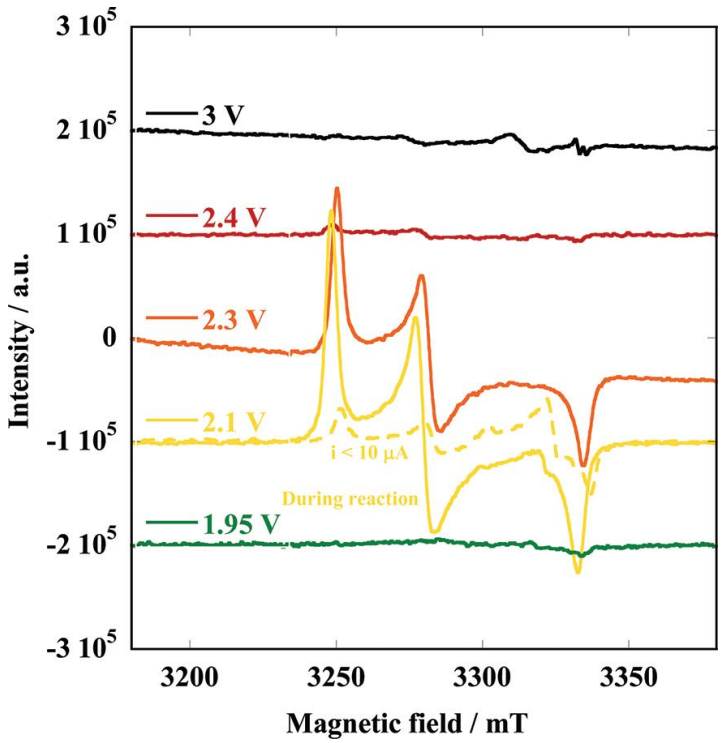

Figure 13 X-band ESR spectra (vertical shifted) obtained at 100 K for catholyte samples after the cell polarization at different potentials. Reprinted with permission from [63]. Copyright (2019) American Chemical Society.

2.4.5 X-ray absorption near-edge structure (XANES).

XANES has been widely used for determining the local geometric or electronic structure of the materials. For the polysulfides species, sulfur K-edge X-ray absorption near-edge structure has been introduced to measure different sulfur compounds, including metal sulfides and polysulfides. The results demonstrate that the pre-edge and sulfur K-edge resonances are sensitive to the sulfur oxidation state. The energy peak location of the sulfur K-edge shifts to a higher position with an about 6 eV between elemental sulfur and sulfate [65]. This property facilitates us to figure out

different oxidation state of sulfur in the Na-S batteries. Meanwhile, the local symmetry of sulfur atoms in the polysulfides possesses a strong impact on the observed shape of the sulfur edge and pre-edge resonances, which could be used as a clue for identifying individual sulfur in the polysulfides species [66]. Recently, Dominko et al. report the application of XANES on detailed analysis of different component in the cathode and separator [67]. The precise results illustrate the relative sulfur amounts in the cathode and separator through the linear combination fit of the XANES spectra based on the reference compounds. The XANES spectra provide us a technique to probe the relative amount Li or Na in Li_2S_x and Na_2S_x species (**Fig.14**), which could help us investigate the mechanism of the PSRFBs system.

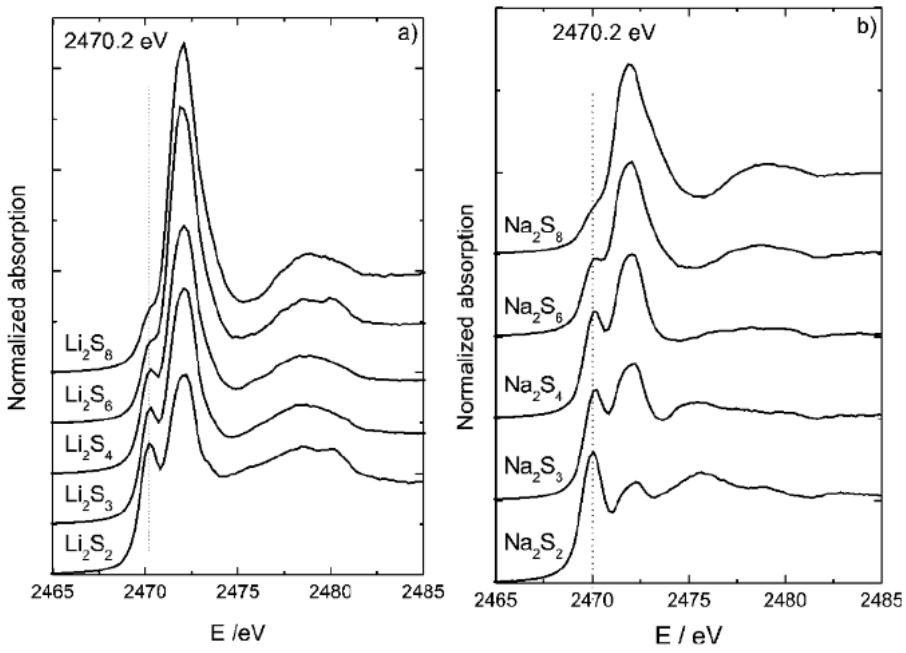

Figure 14 . Sulfur K-edge XANES spectra reveal relative amount Li (a) or Na (b) in Li_2S_x and Na_2S_x species. Spectra are shifted vertically for clarity. Reprinted with permission from [67]

Chapter 3 Material and Experimental

3.1 Material and chemical agents

Anhydrous Na_2S (Sigma-Aldrich, >99%), Na_2S_4 (Beantown Chemical, >90%), and sulfur (Alfa Aesar, 99.5%) are used in this research to synthesize sodium polysulfides. All the above-mentioned chemical agents are argon-packed, and all opened and stored in the argon-filled Glove-box. For the liquid synthesis method, anhydrous ethanol was used as a medium.

The solvent used to dissolve obtained sodium polysulfide products is tetraethylene glycol dimethyl ether (TEGDME, Sigma-Aldrich), the residual water and other impurities in the TEGDME was further removed by molecular sieve, the purified TEGDME was stored in the argon-filled glove-box.

3.2 Equipment

In this research, the muffle furnace (KSL-1100X, MTI corporation) and tube furnace (OTF-1200X, MTI corporation) shown in **Fig.15** were used in the heating synthesis method.

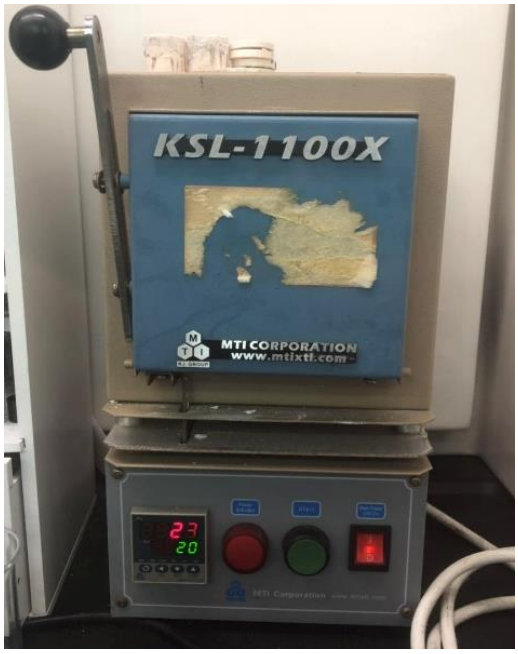

(a)

(b)

Figure 15 Pictures of equipment used in this research (a. Picture of the muffle furnace, b. Picture of the tube furnace.)

3.3 Material characterization

3.3.1 X-ray Diffraction Patterns

Instrumentation

XRD patterns of raw material and sodium polysulfide products in this research were collected using a bench-top X-ray diffractometer (Bruker, D2 PHASER) at a scanning rate of 0.06°/s in the 2θ range from 15° to 80° (Cu Kα radiation, 40kV, 30mA, λ = 1.5418 Å).

Sample preparation:

Due to the air-sensitivity of sodium polysulfides, all sodium polysulfide samples are prepared in the glove box using a zero-diffraction plate with a cavity for XRD (MTI, Si crystal). Firstly, the zero-diffraction plate was cleaned by suitable detergent and ultrasonicated in DI water for 10 minutes, after rinsed by ethanol for several times, it was dried in the oven at 65℃ for more than 1 hour and transfer to the glove-box. Then, placed the sample in the middle of the cavity on the plate, and trimmed the surface of the sample and made it completely flat. Finally, cover the plate and seal the sample in the cavity by Kapton® tape (Dupont).

3.3.2 Raman Spectroscopy

Instrumentation

Raman spectra of all materials and products in this research were collected using a confocal Raman spectrometer (WITec, Alpha 500R). The laser wavelength used in the Raman spectroscopy characterization was 633 nm and the integration time for a single Raman spectrum accumulation

was 1s and accumulated for 5 times. Collected photons were dispersed by a 1200 gr/mm grating, the spectrum center was set to 650 ref. cm^{-1} for solid sample characterization and 800 ref. cm-1 for liquid sample characterization. The 10× objective was used has a laser spot diameter of about 10 μm. The excitation wavelength of the laser was calibrated by a flat silicone plate before spectra collection. For solid samples, Raman spectra of more than 6 random points on the sample were collected. For homogeneous solutions, Raman spectrum of only one point in each solution was collected.

Liquid sample preparation

All liquid samples were prepared in argon-filled glove-box using capillary tubes (Fisher Scientific). The capillary tubes were dried and stored in the oven at 65℃ and transfer to the glove-box. Submerge one end of a capillary tube into the supernatant of each liquid sample and let the liquid flow into it by capillary effect. Seal both two ends of the capillary tube using vacuum grease (Dow Corning).

Solid (powder) sample preparation

Same with liquid sample preparation procedure, all powder samples are prepared in the glove-box using capillary tubes. Firstly, one end of the capillary tube was placed on the flame until this end was sealed. Ultrasonicated above-mentioned of one-end-sealed capillary tubes in ethanol and rinsed using ethanol for several times to remove the impurity on the inner surface near the sealed end, then dried them in the oven at 65℃ for more than 24 hours and transferred prepared capillary tubes to the glove-box.

Tap slightly the open end of the capillary tube in the powder sample to get the sample into the tube, then tap the sealed end slightly to compact the powder sample in the sealed end. Finally, the open end was sealed with vacuum grease.

3.4 Material synthesis

3.4.1 Liquid synthesis method ("Wet" synthesis method)

The apparatus for liquid synthesis method was shown in **Fig.16**. This apparatus consists of a round-bottom flask, a reflux condenser, a glycerin bath, and a heater. Meanwhile, argon was used as a protecting gas, the reaction in the round-bottom flask can be protected from reacting with the air by the argon passing through the solution. Firstly, a solution of Na_2S_4 in anhydrous ethanol was prepared and placed in a round-bottom flask. Removed the reflux condenser, added stoichiometric fresh metal sodium into the solution, then put back the reflux condenser rapidly. The mixture was heated at 80℃ for 30 min. According to the method recorded in Courtois' study [47], a light yellow precipitate of sodium disulfide can be obtained by this reaction, and after removing the solvent by filtration and washing by absolute ethanol, a relatively pure Na_2S_2 can be obtained.

Figure 16 Apparatus for the preparation of Na_2S_2 by liquid synthesis method

3.4.2 Heating synthesis method (“Dry” synthesis method)

Atmospheric pressure heating synthesis

Al_2O_3 crucibles used for atmospheric pressure heating were cleaned by ethanol, then roasted at 1000℃ for more than 2 hours to further remove the impurity on the surface of crucibles and store the crucibles in the oven at 65℃. As shown in **Fig.17,** the mixtures of sodium sulfide and sulfur should be sealed in crucibles. Firstly, the vacuum grease was smeared on the covers of the crucibles, and crucibles and covers were transported into the glove-box. Then, 0.50g of sodium sulfide and the stoichiometric amount of sulfur powder was gathered and sealed in each alumina crucible. The

crucibles with mixture should be sealed with ceramic glue again when they were taken out from the glove-box. After the ceramic glue dried thoroughly, crucibles were rolled and shake to well mix the Na_2S and sulfur in them. The prepared samples were roasted in the muffle furnace according to the certain heating procedure. Several heating procedure settings were tried out and will be illustrated in detail in Chapter 4.

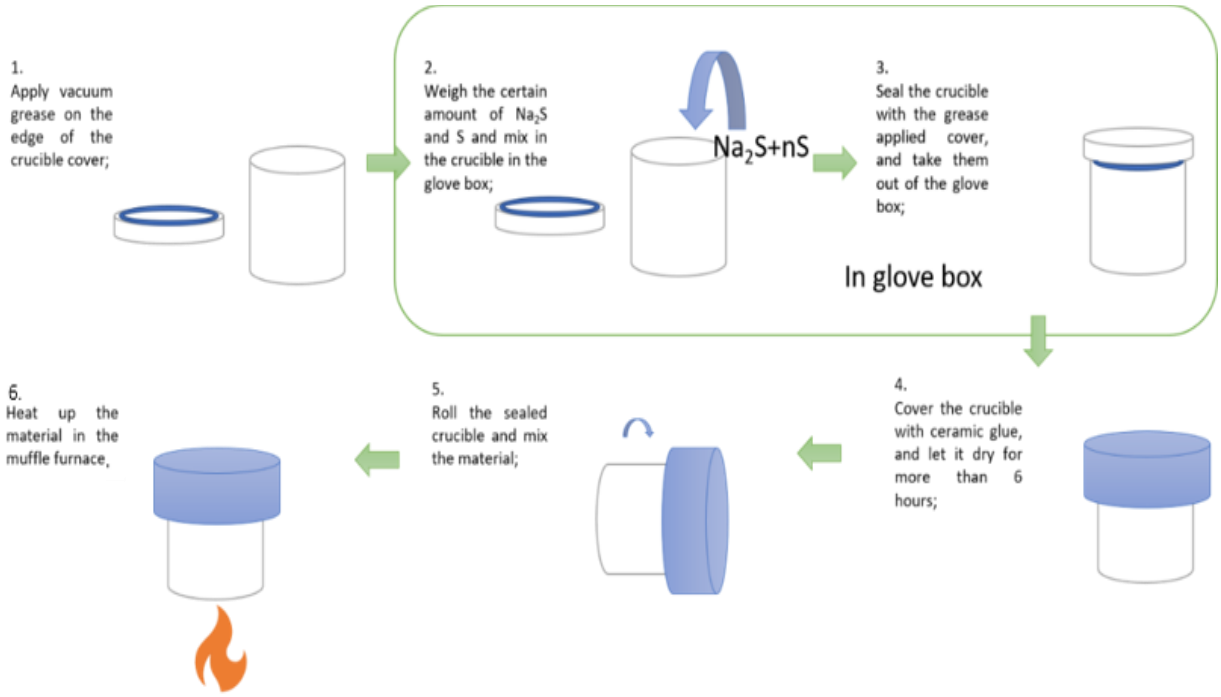

Figure 17 *Schematic for the atmospheric-pressure heating synthesis*

Vacuum heating synthesis

At first, the vacuum heating was conducted in the tube furnace connected to a vacuum pump. Before transfer to the glove-box, the samples were prepared by a similar procedure for atmospheric-pressure heating synthesis and sealed in the crucibles by vacuum grease in the glove-box. The crucible was transferred with a sample from the glove-box and placed it in the middle of

the tube furnace, then vacuumed the tube furnace and roast the sample according to the certain heating procedure.

Revised vacuum heating synthesis

Due to the evaporation of sulfur, the vacuum heating method was revised. As shown in **Fig.18**, 0.50g Na_2S and the stoichiometric amount of sulfur was combined and ground in the agate mortar and gathered in the bottom of a quartz tube using a long-neck funnel. The open end of the quartz tube was sealed by the Teflon tape temporarily, then, connected to vacuum line after the quartz tube was transferred out of the glove box, and sealed by high-temperature oxyhydrogen flame after the tube was vacuumed to 10^{-6} torr. The prepared vacuumed quartz tubes were roasted in the muffle furnace, the heating procedure will be shown in Chapter 4.

1) Weighed the reactants;

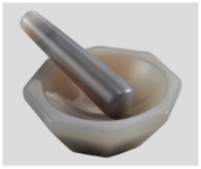

2) Combined the reactants;

3) Transferred reactants to the quartz and pressed the mixture to the bottom of the tube;

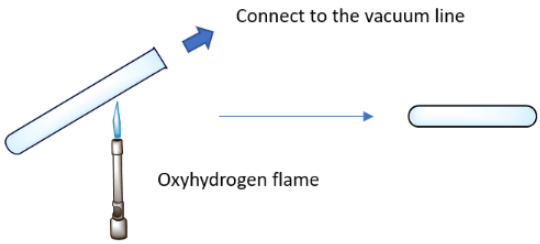

4) Vacuumed and sealed the quartz tube.

(a)

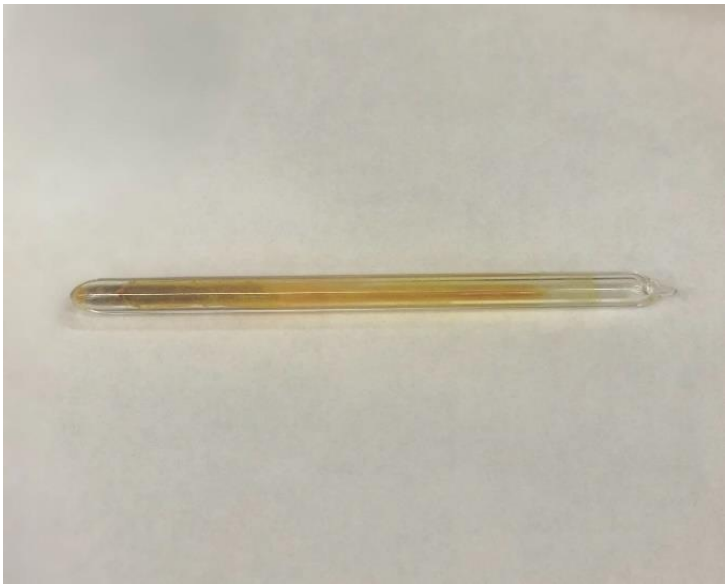

(b)

Figure 18 Preparation of samples for revised heating synthesis method (a. Preparation procedure of the samples, b. Picture of the sample sealed in the vacuum quartz tube.)

2.5 Preparation of sodium polysulfide solution in TEGDME

To study the influence of electrolyte solvent on the sodium polysulfides. The amount of each polysulfide to prepare 0.25M solution in TEGDME was added into the TEGDME solvent, and the mixtures were placed on the stirring table overnight. The supernatant of the solution of each polysulfide was analyzed by Raman spectroscopy.

Chapter 4 Result and Discussion

4.1 Feasibility of "wet" synthesis method

In contrast with the phenomena recorded in Courtois's study [47], the Na_2S_4 cannot dissolve in the ethanol solvent thoroughly. The metal sodium pieces added into the solution reacted with ethanol rapidly. There was no obvious color change happening to the solution and the undissolved Na_2S_4 precipitation during the heating process. And the precipitate obtained was dried and characterized by XRD. As shown in **Fig.19**, the precipitate mainly consists of Na_2S_4 and some unknown impurities and there was no peak belonging to Na_2S_2 observed in the XRD pattern.

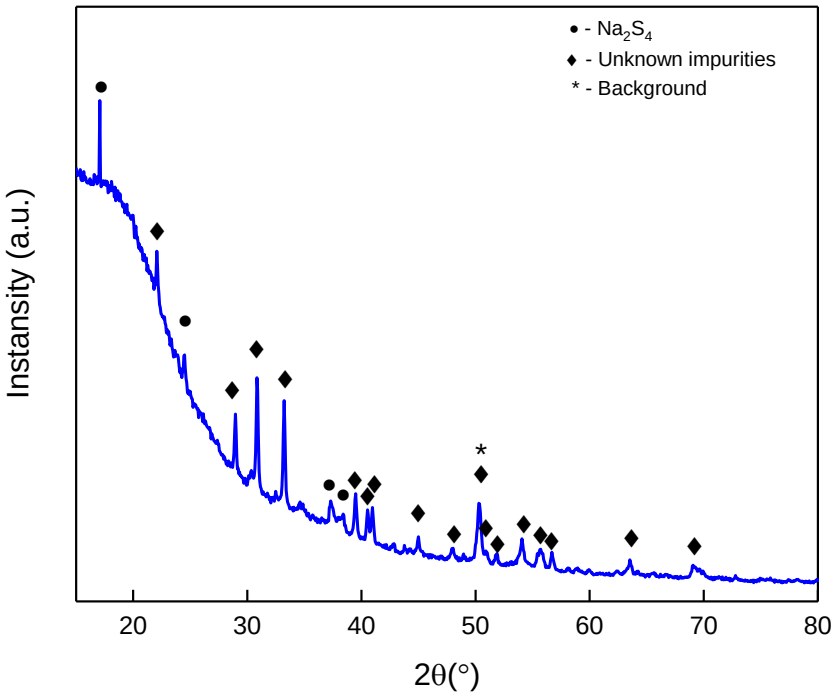

Figure 19 XRD pattern of the precipitate obtained in the ethanol

4.2 Feasibility of “dry” synthesis methods

4.2.1 Feasibility of atmospheric pressure heating synthesis

The sample was prepared as the method illustrated in Chapter 3. According to the heating procedures reported [10, 68], mixtures (with the S/Na_2S ratio of 0.5, 1, 2, 3, 4, 5) roasted at 400℃ for 2 hours, after that, melted at 600 for 1 hour and annealed at 200℃ for 6 hours, then cooled down to room temperature slowly.

According to the XRD pattern of the products (shown in **Fig.20**, only Na_2S_4 can be obtained by this method, which is coincident with the Na-S phase diagram with isobar of the partial pressure of sulfur (shown in **Fig.9**), at atmospheric pressure, only Na_2S_4 phase can be generated when heated to above 400℃.

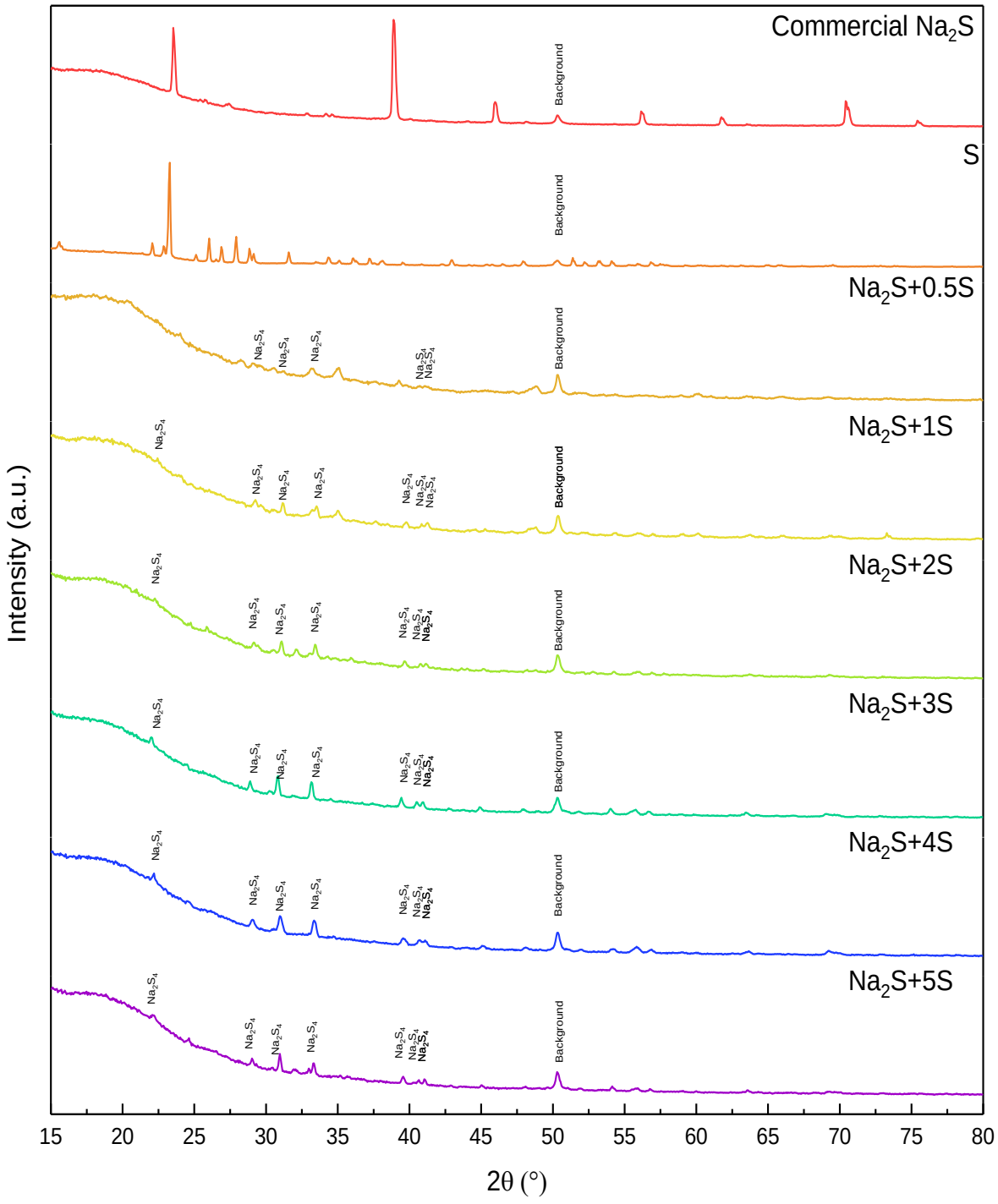

Figure 20 XRD patterns of products with different S/Na_2S ratio by heated at atmospheric pressure

4.2.2 Feasibility of vacuum heating synthesis

By this method, the mixture with the S/Na_2S ratio of 1 was heated by the same heating process of atmospheric-pressure heating**.** According to the XRD pattern of the product shown in **Fig.21**, by vacuum heating, Na_2S_2 can be generated, which meets the Na-S phase diagram. However, it is difficult to control the real ratio of the reactants by this method because of the evaporation of sulfur during heating, hence, it is hard to obtain relatively pure sodium polysulfide phase by this method.

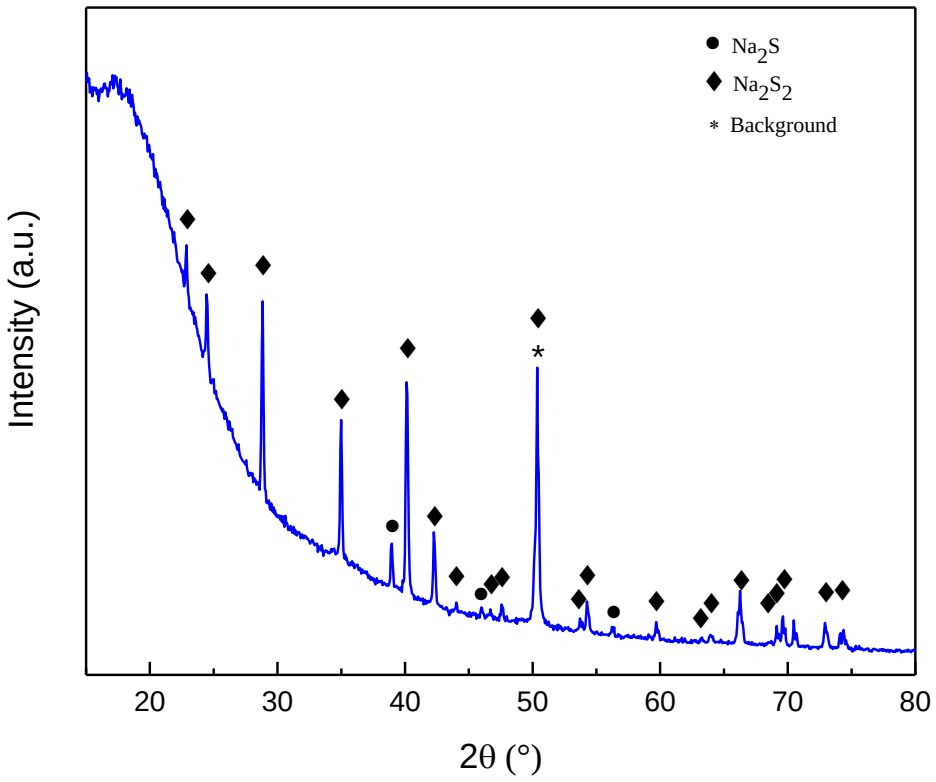

Figure 21 XRD pattern of vacuum heating synthetic product

4.2.3 Feasibility of revised vacuum heating synthesis

To avoid the influence caused by the evaporation of sulfur, the vacuum heating synthesis method was revised. The mixtures of the precursors were sealed in vacuum quartz tubes, by the former heating process. By this method and heating process, a relatively pure Na_2S_2 can be obtained, the XRD pattern and Raman spectra of the Na_2S_2 product will be shown in 4.3.2.

However, Na_2S_5 cannot be obtained by the same heating process, the XRD pattern of the product obtained by this heating process was shown in **Fig.22**. According to this figure, when the sample with a S/Na_2S ratio of 4 was prepared and heated by the same procedure, an amorphous product was obtained. According to the Na-S phase diagram, the melting point of Na_2S_5 is much lower than that of Na_2S_2, the annealing temperature for Na_2S_2 might be too high for the synthesis of Na_2S_5 and not benefit for the crystal growth for Na_2S_5. Hence, the heating process was revised, the precursor was heated at 400℃ for more than 2h to make sure sodium sulfide and sulfur can react completely and melt at 600℃. Then the roasted sample was cooled down slowly, annealed at 200℃ and 100 ℃ in sequence for 5h respectively. By this revised heating process, a relatively pure Na_2S_5 can be obtained, the characterization of this product will be shown in 4.3.4**.**

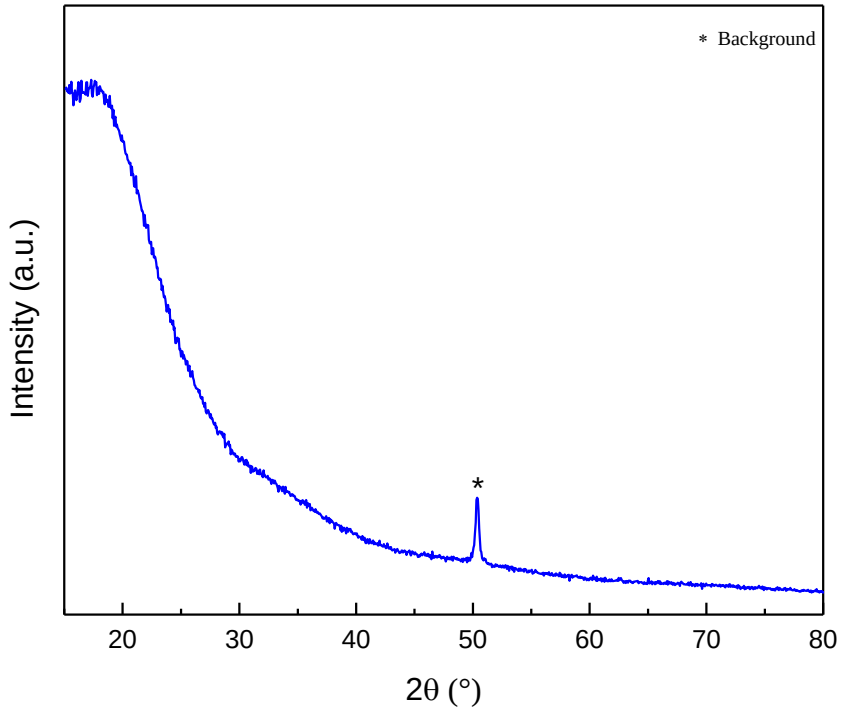

Figure 22 XRD pattern of vacuum heating products with S/Na_2S ratio of 4 and annealing temperature of 200℃

4.3 Sodium polysulfides and their characterization.

4.3.1 Na_2S and its characterization

Na_2S is a white crystalline compound, the picture of the Na_2S obtained from Sigma-Aldrich was shown in **Fig.23a**, and the XRD pattern and the Raman spectrum of it were shown in **Fig.23b** and **23c**, respectively. According to **Fig.23b** and **23c**, commercial Na_2S is in very high purity.

(a)

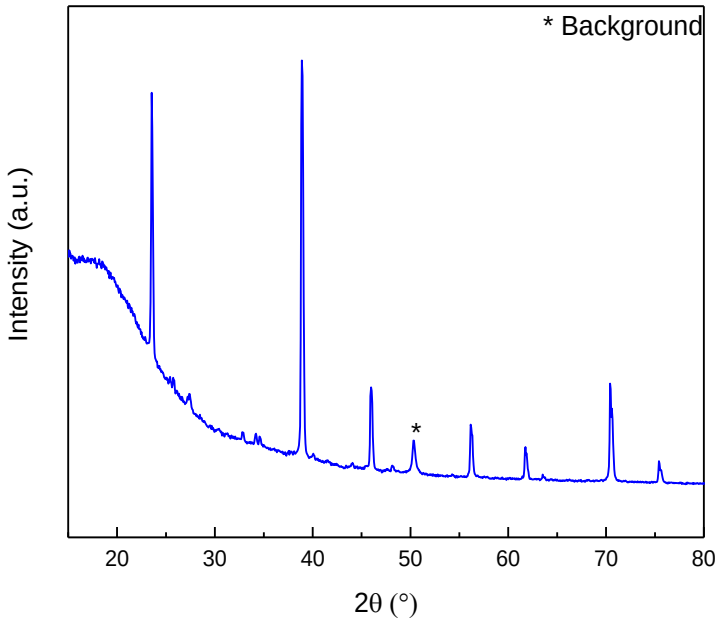

(b)

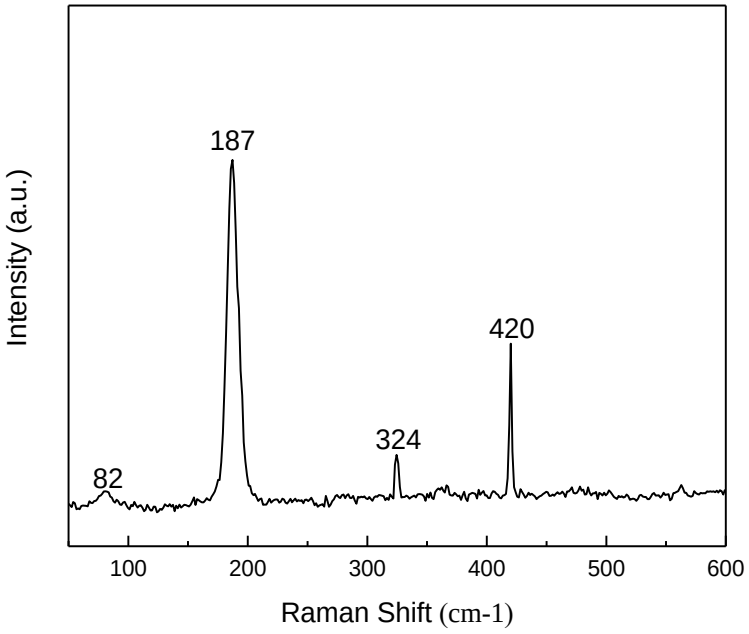

(c)

Figure 23 Picture (a), XRD pattern (b) and Raman spectrum (c) of Na_2S

4.3.2 Na_2S_2 and its characterization

As shown in **Fig.24a**, the Na_2S_2 obtained by the revised vacuum heating synthesis method is light yellow, very hygroscopic powder. According to the XRD pattern of the product shown in **Fig.24b**, the product mainly consists of Na_2S_2, and there is also a slight amount of Na_2S residue in it. And according to the Raman spectrum of the product (shown in **Fig.24c)**, the solid phase of Na_2S_2 can be characterized by the S-S stretching band at 450 cm^{-1} and S_2^{2-} liberational band at 133 cm^{-1} [68], only bands belong to Na_2S_2 can be observed in the Raman spectrum.

(a)

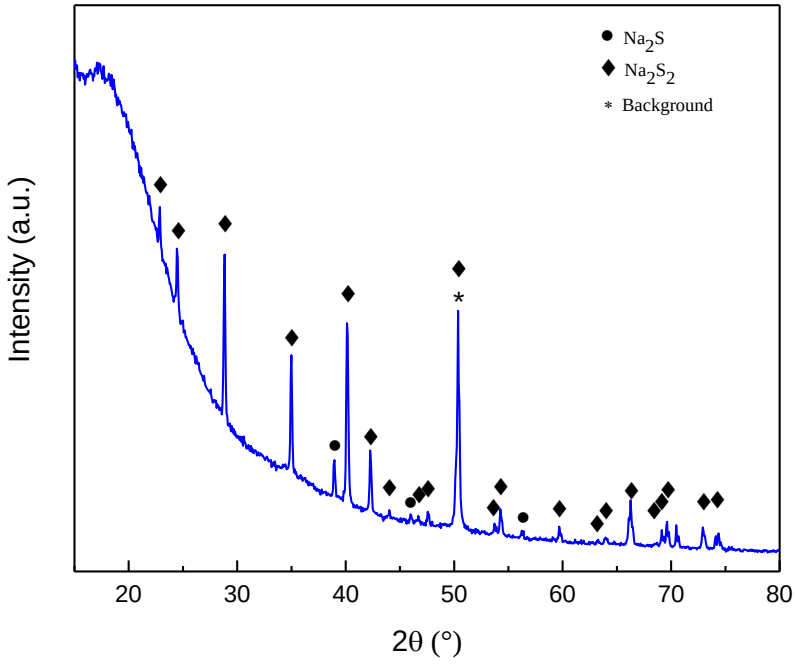

(b)

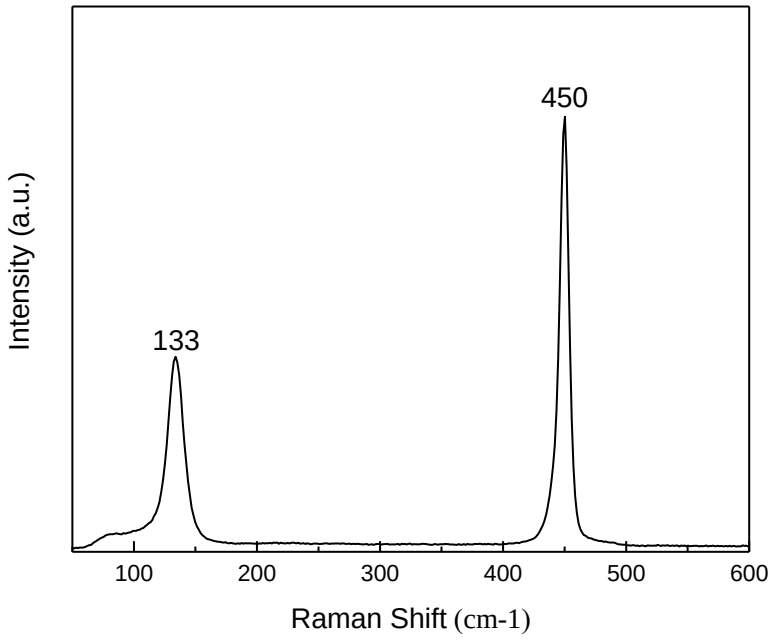

(c)

Figure 24 Picture (a), XRD pattern (b) and Raman spectrum (c) of Na_2S_2

4.3.3 Na_2S_4 and its characterization

Na_2S_4 (>90%) can be obtained from the Beantown Chemical Company is a hygroscopic grayish-yellow powder, the photo of the Na_2S_4 powder was shown in **Fig.25a**. The XRD pattern shown in **Fig.25b** shows that there are some unknown impurities in the commercial Na_2S_4. The Raman spectrum of the commercial Na_2S_4 was shown in **Fig.25c**, bands that have been reported belong to Na_2S_4 was labeled in the figure, according to the figure, most of the bands that can be observed in the spectrum belong to Na_2S_4 [68-71].

(a)

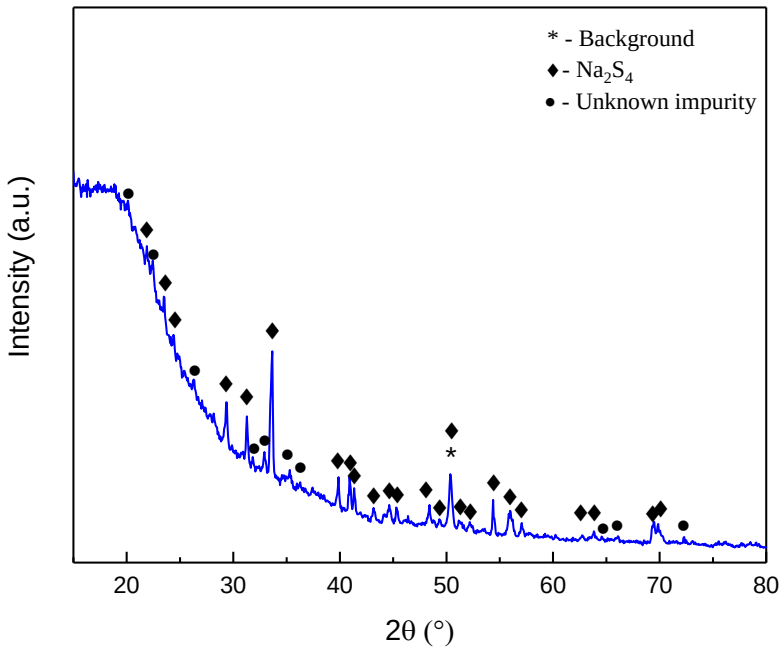
* - Background
♦- Na2S4
● - Unknown impurity
Intensity (a.u.)
20
30
40
50
60
70
80
2θ (°)

(b)

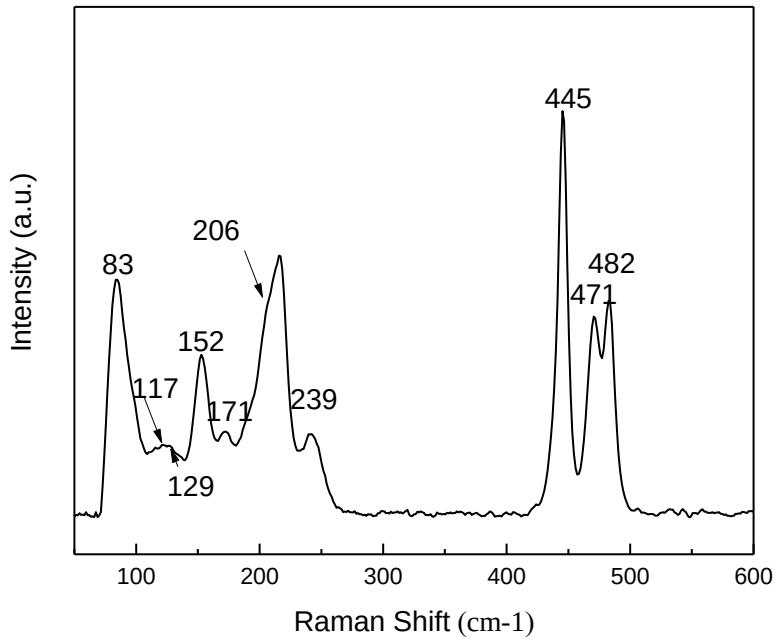

(c)

Figure 25 Picture (a), XRD pattern (b) and Raman spectrum (c) of Na_2S_4

4.3.4 Na_2S_5 and its characterization

The revised annealing process allowed the crystal growth of Na_2S_5. As shown in **Fig.26a**, the Na_2S_5 obtained is very hygroscopic yellowish-brown powder. According to the XRD pattern of the product shown in **Fig.26b**, this product mainly consists of Na_2S_5. And according to the Raman spectrum of the product (shown in **Fig.26c**), the solid phase of Na_2S_5 can be characterized by the stretching bands at 391 cm^{-1}, 429 cm^{-1}, 444 cm^{-1} and 488 cm^{-1}, bending bands at 214 cm^{-1} and 266 cm^{-1}, and torsional bands at 103 cm^{-1} and 135 cm^{-1} [68]. All bands can be obviously observed in the Raman spectrum belong to Na_2S_5.

(a)

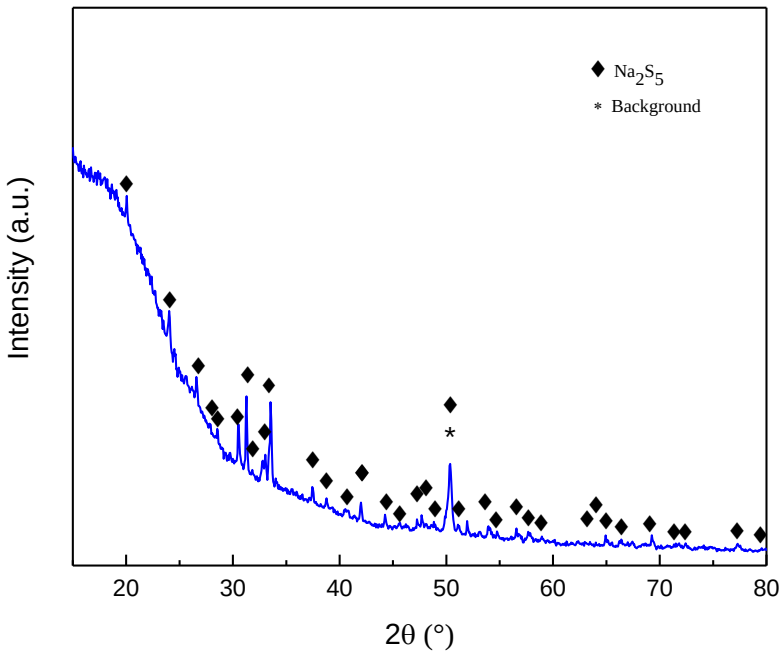

(b)

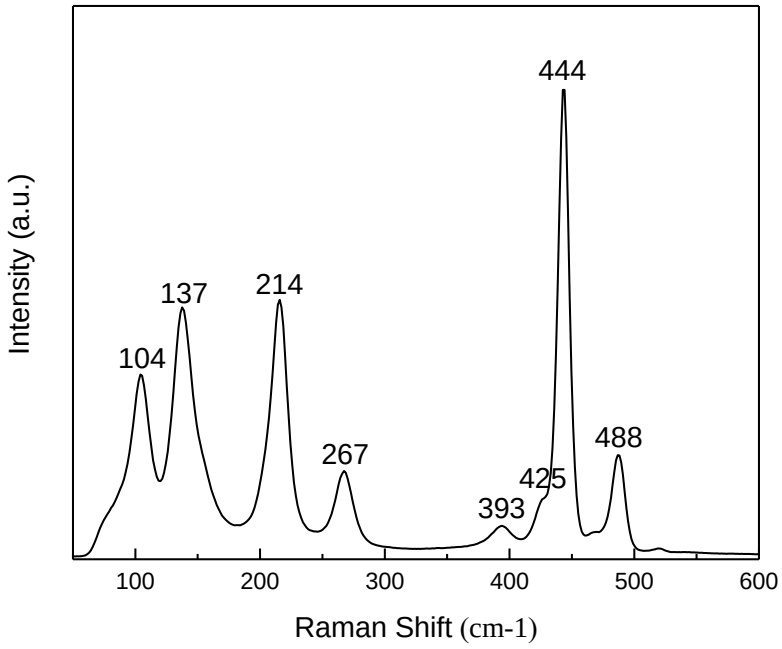

(c)

Figure 26 Picture (a), XRD pattern (b) and Raman spectrum (c) of Na_2S_5

4.4 Na_2S_n in TEGDME

The solution of Na_2S_n in TEGDME was prepared. For each sample, an amount to prepare a 0.25M solution was used. The picture of the prepared solutions was shown in **Fig.27**. Na_2S can hardly dissolve in TEGDME, and the supernatant is a colorless liquid. Na_2S_2 is slightly soluble in the TEGDME, and the color of the supernatant is transparent green. Na_2S_4 can dissolve in TEGDME and has a much larger solubility than Na_2S and Na_2S_2, the supernatant shows color of brownish-green. Na_2S_5 can easily dissolve in TEGDME, and the color of the solution turns to yellowish-brown. The color of Na_2S_n TEGDME solutions prepared by Na_2S_n compounds is obviously different with solutions prepared by the stoichiometrically mixed Na_2S and S in Kim et al.'s

research [25], each solution in their research shows a higher solubility and a longer-wavelength color than the corresponding solution in this research. Solutions prepared by the Na_2S_n compounds can act as better standard references for the mechanism study of Na-S battery.

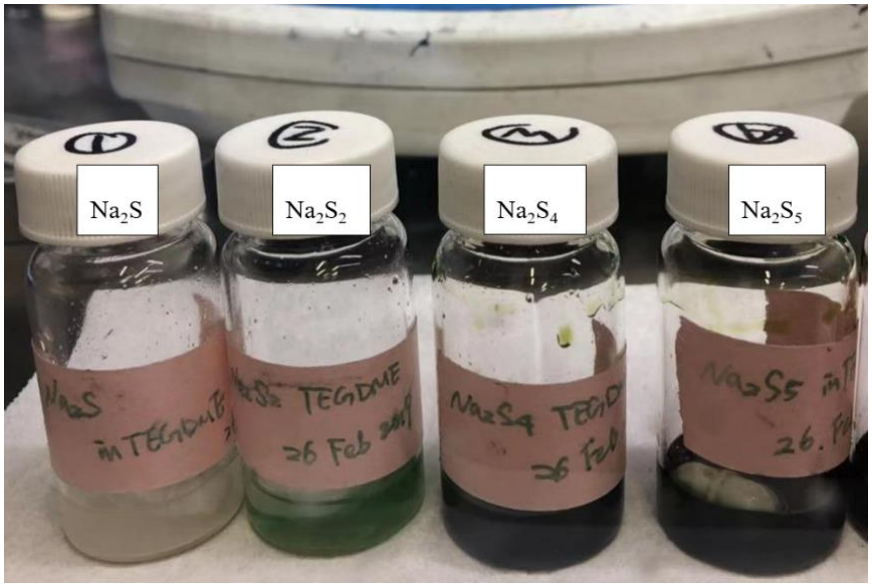

Figure 27 Picture of Na_2S_n solution prepared by TEGDME

The supernatant of each solution was characterized by Raman spectroscopy, and the Raman spectra of the supernatants were shown in the following figure. Due to the low solubility of Na_2S, there was no obvious band can be found in the supernatant of Na_2S in TEGDME. And in the supernatant of Na_2S_2 in TEGDME, the dissolved Na_2S_2 reacted with TEGDME and generated S_3^{2-} (band at 532 cm^{-1}) and $S_2O_4^{2-}$ (band at 1066 cm^{-1}) [72]. The components in the supernatants of Na_2S_4 and Na_2S_5 are almost the same, dissolved Na_2S_4 and Na_2S_5 forms S_4^{2-} (band at 233 cm^{-1}), S_6^{2-} (band at 299cm^{-1}) ,S_3^{2-} (band at 532 cm^{-1}), S_x^{2-} (x=4-8,band at 766 cm^{-1}), $S_2O_4^{2-}$ (band at 1066 cm^{-1}) [72, 73]. $S_2O_4^{2-}$ might be generated by the reaction of sodium polysulfide and the TEGDME.

Hence, the color difference among these Na_2S_n solutions in TEGDME might be due to the different polysulfide anions that exist in the solution. The intensity of each band increased with the increasing sulfur containing in sodium polysulfides, which might be because of the increased amount of the dissolved sodium polysulfide in corresponding supernatants. The Raman spectra of the Na_2S_n in the TEGDME can be used to determine the discharged product in the cathode for the in-situ Raman study of the TEGDME of Na-S battery.

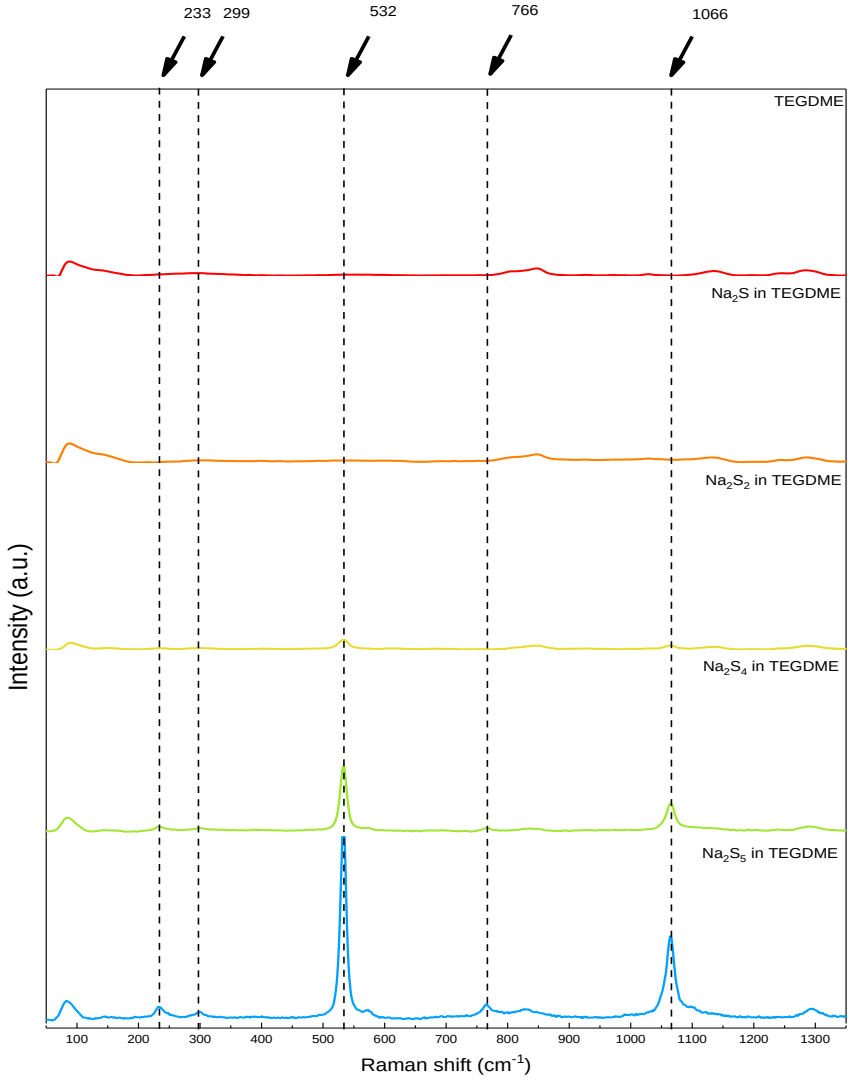

Figure 28 Raman spectra the supernatants of Na_2S_n in TEGDME

Chapter 5 Conclusion and Future Works

5.1 Conclusion

This research examined several reported synthesis methods for sodium polysulfide reported and revised the synthesis method and process for Na_2S_2 and Na_2S_5. After that, the commercial and obtained sodium polysulfides was dissolved in TEGDME, their properties in TEGDME were studied in this thesis.

1) Na_2S_2 cannot be obtained by the liquid synthesis method using anhydrous ethanol as media for the reaction of Na_2S and S;
2) Only Na_2S_4 can be generated by the reaction of Na_2S and sulfur when the mixture of Na_2S and S (S/Na_2S=0.5, 1, 2, 3…) at atmospheric pressure;
3) Na_2S_2 and Na_2S_5 can be obtained by the vacuum heating synthesis, Na_2S and S should be sealed in the vacuumed container to avoid the evaporation of sulfur during the synthesis;
4) For the synthesis of Na_2S_2, Na_2S and S were mixed with a ratio of 1:1 and sealed in a vacuum quartz tube, the sample was roasted in a muffle furnace, after heating the precursor at 400℃ for 2 hours and melting it at 600℃ to homogeneous for 1 hour, the sample should be annealed at 200℃ for 6 hours and cooled down to room temperature slowly to benefit the crystal growth of Na_2S_2 product;
5) For the synthesis of Na_2S_5, the annealing temperature should be decreased due to the crystallizing points of Na_2S_2 and Na_2S_5. Na_2S and S were mixed with a ratio of 1:4 and sealed in the vacuum quartz tube, the sample was roasted in a muffle furnace, after heating the precursor at 400℃ for 2 hours and melting it at 600℃ to homogeneous for 1 hour as

the heating process for the synthesis of Na_2S_2, the sample should be annealed at 200℃ and 100℃ in sequence for 5 hours respectively and cooled down to room temperature slowly.

6) Na_2S can hardly dissolve in TEGDME, and the supernatant is a colorless liquid. Na_2S_2 is slightly soluble in the TEGDME, and the color of the supernatant is transparent green. Na_2S_4 can dissolve in TEGDME and has a much larger solubility than Na_2S and Na_2S_2, the supernatant shows color of brownish-green. Na_2S_5 can easily dissolve in TEGDME, and the color of the solution gets to yellowish-brown.
7) Dissolved Na_2S_n reacted with TEGDME, for Na_2S_2, only short-chain polysulfide anion, S_3^{2-}, can be observed. With the increase of the sulfur-containing in Na_2S_n, the long-chain polysulfide anions were generated in the solution.

5.2 Future works

Commercial sodium polysulfides and the synthetic sodium polysulfides obtained in this thesis will be used to prepare cathodes to study the lower-voltage-plateau region of Na-S batteries avoiding the influence of the transformation of S_8 to polysulfide anions. Na_2S_n will be combined with carbon black and PTFE by a ratio of 2:2:1 by a dry-blending process and several common electrolytes will be applied in cells. This research might be able to determine the most stable discharge product in the cathode of Na-S energy storage systems and offer helpful information to increase the reversibility of the Na-S batteries. Meanwhile, sodium polysulfide will be dissolved in several other common electrolytes and used as standard references for in-situ study of the Na-S battery system.

References:

1. Yao, Y.-F.Y. and J. Kummer, *Ion exchange properties of and rates of ionic diffusion in beta-alumina.* Journal of Inorganic and Nuclear Chemistry, 1967. **29**(9): p. 2453-2475.
2. South, K., J. Sudworth, and J. Gibson, *Electrode Processes in Sodium Polysulfide Melts.* Journal of The Electrochemical Society, 1972. **119**(5): p. 554-558.
3. Ellis, B.L. and L.F. Nazar, *Sodium and sodium-ion energy storage batteries.* Current Opinion in Solid State and Materials Science, 2012. **16**(4): p. 168-177.
4. Park, C.-W., et al., *Room-Temperature Solid-State Sodium/ Sulfur Battery.* Electrochemical and solid-state letters, 2006. **9**(3): p. A123-A125.
5. Cheng, F., et al., *Functional Materials for Rechargeable Batteries.* Advanced Materials, 2011. **23**(15): p. 1695-1715.
6. Malik, R., F. Zhou, and G. Ceder, *Kinetics of non-equilibrium lithium incorporation in LiFePO 4.* Nature materials, 2011. **10**(8): p. 587.
7. Zhu, Y., et al., *Carbon-based supercapacitors produced by activation of graphene.* science, 2011. **332**(6037): p. 1537-1541.
8. Li, J.-T., et al., *In-situ infrared spectroscopic studies of electrochemical energy conversion and storage.* Accounts of chemical research, 2012. **45**(4): p. 485-494.
9. Li, Z., et al., *Air-breathing aqueous sulfur flow battery for ultralow-cost long-duration electrical storage.* Joule, 2017. **1**(2): p. 306-327.
10. Bruce, P.G., et al., *Li–O2 and Li–S batteries with high energy storage.* Nature Materials, 2011. **11**: p. 19.
11. Song, M.-K., E.J. Cairns, and Y. Zhang, *Lithium/sulfur batteries with high specific energy: old challenges and new opportunities.* Nanoscale, 2013. **5**(6): p. 2186-2204.
12. Yang, Z., et al., *Enabling renewable energy—and the future grid—with advanced electricity storage.* Jom, 2010. **62**(9): p. 14-23.
13. Zhu, J., et al., *High energy batteries based on sulfur cathode.* Green Energy & Environment, 2018.
14. Yu, X. and A. Manthiram, *Room-temperature sodium–sulfur batteries with liquid-phase sodium polysulfide catholytes and binder-free multiwall carbon nanotube fabric electrodes.* The Journal of Physical Chemistry C, 2014. **118**(40): p. 22952-22959.
15. Available from: http://en.wikipedia.org/wiki/File:Elemental_abundances.svg
16. Oshima, T., M. Kajita, and A. Okuno, *Development of sodium-sulfur batteries.* International Journal of Applied Ceramic Technology, 2004. **1**(3): p. 269-276.
17. Wen, Z., et al., *Research on sodium sulfur battery for energy storage.* Solid State Ionics, 2008. **179**(27-32): p. 1697-1701.

18. Sarasua, A., et al. *Modelling of NAS energy storage system for power system applications*. in *2010 IEEE/PES Transmission and Distribution Conference and Exposition: Latin America (T&D-LA)*. 2010. IEEE.

19. Ji, X., K.T. Lee, and L.F. Nazar, *A highly ordered nanostructured carbon–sulphur cathode for lithium–sulphur batteries.* Nature materials, 2009. **8**(6): p. 500.

20. Ji, X., et al., *Stabilizing lithium–sulphur cathodes using polysulphide reservoirs.* Nature communications, 2011. **2**: p. 325.

21. He, G., X. Ji, and L. Nazar, *High "C" rate Li-S cathodes: sulfur imbibed bimodal porous carbons.* Energy & Environmental Science, 2011. **4**(8): p. 2878-2883.

22. Xin, S., et al., *A high-energy room-temperature sodium-sulfur battery.* Advanced Materials, 2014. **26**(8): p. 1261-1265.

23. Hayashi, A., et al., *All-solid-state Li/S batteries with highly conductive glass–ceramic electrolytes.* Electrochemistry communications, 2003. **5**(8): p. 701-705.

24. Yu, X. and A. Manthiram, *Ambient-Temperature Sodium–Sulfur Batteries with a Sodiated Nafion Membrane and a Carbon Nanofiber-Activated Carbon Composite Electrode.* Advanced Energy Materials, 2015. **5**(12): p. 1500350.

25. Kim, I., et al., *Sodium polysulfides during charge/discharge of the room-temperature Na/S battery using TEGDME electrolyte.* Journal of The Electrochemical Society, 2016. **163**(5): p. A611-A616.

26. Bauer, I., et al., *Shuttle suppression in room temperature sodium–sulfur batteries using ion selective polymer membranes.* Chemical Communications, 2014. **50**(24): p. 3208-3210.

27. Park, C.-W., et al., *Discharge properties of all-solid sodium–sulfur battery using poly (ethylene oxide) electrolyte.* Journal of power sources, 2007. **165**(1): p. 450-454.

28. Kim, J.-S., et al., *The short-term cycling properties of Na/PVdF/S battery at ambient temperature.* Journal of Solid State Electrochemistry, 2008. **12**(7-8): p. 861-865.

29. Wang, X., et al., *Sulfur covalently bonded graphene with large capacity and high rate for high-performance sodium-ion batteries anodes.* Nano Energy, 2015. **15**: p. 746-754.

30. Kim, I., et al., *A singular flexible cathode for room temperature sodium/sulfur battery.* Journal of Power Sources, 2016. **307**: p. 31-37.

31. Fan, L., et al., *Covalent sulfur for advanced room temperature sodium-sulfur batteries.* Nano Energy, 2016. **28**: p. 304-310.

32. Ryu, H., et al., *Discharge reaction mechanism of room-temperature sodium–sulfur battery with tetra ethylene glycol dimethyl ether liquid electrolyte.* Journal of Power Sources, 2011. **196**(11): p. 5186-5190.

33. Yu, X. and A. Manthiram, *Capacity Enhancement and Discharge Mechanisms of Room-Temperature Sodium–Sulfur Batteries.* ChemElectroChem, 2014. **1**(8): p. 1275-1280.

34. Wei, S., et al., *A stable room-temperature sodium–sulfur battery.* Nature communications, 2016. **7**: p. 11722.

35. Wang, Y.X., et al., *Room-temperature sodium-sulfur batteries: a comprehensive review on research progress and cell chemistry.* Advanced Energy Materials, 2017. **7**(24): p. 1602829.

36. Janz, G. and D. Rogers, *Melting-crystallization properties of the sulphur electrolyte in sodium-sulphur batteries.* Journal of Applied Electrochemistry, 1983. **13**(1): p. 121-131.

37. Friedrich, K. and M. Waehlert, *Investigation of layer-forming systems.* Metall und Erz, 1914: p. 160-167.

38. Rule, A. and J.S. Thomas, *XXIII.—The polysulphides of the alkali metals. Part I. The polysulphides of sodium.* Journal of the Chemical Society, Transactions, 1914. **105**: p. 177-189.

39. Thomas, J.S. and A. Rule, *The Polysulfides of the Alkali Metals.* Journal Chemical Soc., Part, 1917. **3**: p. 1063.

40. Pearson, T.G. and P.L. Robinson, *CLXXXIX.—The polysulphides of the alkali metals. Part I. Sodium (i).* Journal of the Chemical Society (Resumed), 1930: p. 1473-1497.

41. Tegman, R., *THERMODYNAMIC STUDIES OF HIGH-TEMPERATURE EQUILIBRIA. 11. TEMPERATURE-DEPENDENCE OF EQUILIBRIA BETWEEN SULFUR VAPOR AND SPECIES IN SODIUM POLYSULFIDE MELTS.* Chemica Scripta, 1976. **9**(4): p. 158-166.

42. Sangster, J. and A. Pelton, *The Na-S (sodium-sulfur) system.* Journal of phase equilibria, 1997. **18**(1): p. 89-96.

43. Yu, X. and A. Manthiram, *Na2S–Carbon Nanotube Fabric Electrodes for Room-Temperature Sodium–Sulfur Batteries.* Chemistry–A European Journal, 2015. **21**(11): p. 4233-4237.

44. Manan, N.S., et al., *Electrochemistry of sulfur and polysulfides in ionic liquids.* The Journal of Physical Chemistry B, 2011. **115**(47): p. 13873-13879.

45. Rengade, E. and N. Costeanu, *On the Anhydrous Monosulfides of the Alkali Metals.* CR Hebd. Séances Acad. Sci., 1913. **156**: p. 791-793.

46. Klemm, W., H. Sodomann, and P. Langmesser, *Beiträge Zur Kenntnis der Alkalimetallchalkogenide.* Zeitschrift für anorganische und allgemeine Chemie, 1939. **241**(2-3): p. 281-304.

47. Courtois, G., *Preparation of Anhydrous Sodium Sulfide.* CR Hebd. Seances Acad. Sci, 1938. **207**: p. 1220-1221.

48. Bailar, J.C. and A. Trotman-Dickenson, *Comprehensive inorganic chemistry*. Vol. 3. 1973: Pergamon press Oxford.

49. Mali, G., et al., *Stable Crystalline Forms of Na Polysulfides: Experiment versus Ab Initio Computational Prediction.* Chemistry–A European Journal, 2016. **22**(10): p. 3355-3360.

50. Rosen, E. and R. Tegman, *A preparative and X-ray powder diffraction study of the polysulfides Na2S2, Na2S4, and Na2S5.* Acta Chem. Scand, 1971. **25**: p. 3329-3336.

51. Yeon, J.-T., et al., *Raman spectroscopic and X-ray diffraction studies of sulfur composite electrodes during discharge and charge.* Journal of The Electrochemical Society, 2012. **159**(8): p. A1308-A1314.

52. Hagiwara, H., W.J. Suszynski, and L.F. Francis, *A Raman spectroscopic method to find binder distribution in electrodes during drying.* Journal of Coatings Technology and Research, 2014. **11**(1): p. 11-17.

53. Balbuena, P.B. and Y. Wang, *Lithium-ion batteries: solid-electrolyte interphase*. 2004: Imperial college press.

54. Hardwick, L.J., et al., *In situ Raman spectroscopy of insertion electrodes for lithium-ion batteries and supercapacitors: First cycle effects.* Journal of Physics and Chemistry of Solids, 2008. **69**(5-6): p. 1232-1237.

55. Khan, S.A., R.W. Hughes, and P.A. Reynolds, *Raman spectroscopic determination of oxoanions in aqueous polysulfide electrolyte solutions.* Vibrational Spectroscopy, 2011. **56**(2): p. 241-244.

56. Lu, X., et al., *Advanced intermediate-temperature Na–S battery.* Energy & Environmental Science, 2013. **6**(1): p. 299-306.

57. Dillard, C., A. Singh, and V. Kalra, *Polysulfide Speciation and Electrolyte Interactions in Lithium–Sulfur Batteries with in Situ Infrared Spectroelectrochemistry.* The Journal of Physical Chemistry C, 2018. **122**(32): p. 18195-18203.

58. Yue, L., et al., *Highly hydroxylated carbon fibres as electrode materials of all-vanadium redox flow battery.* Carbon, 2010. **48**(11): p. 3079-3090.

59. Lawton, J.S., et al., *Qualitative behavior of vanadium ions in Nafion membranes using electron spin resonance.* Journal of membrane science, 2013. **428**: p. 38-45.

60. Vijayakumar, M., et al., *Spectroscopic investigations of the fouling process on Nafion membranes in vanadium redox flow batteries.* Journal of membrane science, 2011. **366**(1-2): p. 325-334.

61. Kamyshny, A., et al., *Method for the determination of inorganic polysulfide distribution in aquatic systems.* Analytical chemistry, 2006. **78**(8): p. 2631-2639.

62. Rizkov, D., et al., *Development of in-house reference materials for determination of inorganic polysulfides in water.* Accreditation and quality assurance, 2004. **9**(7): p. 399-403.

63. Barchasz, C., et al., *Lithium/sulfur cell discharge mechanism: an original approach for intermediate species identification.* Analytical chemistry, 2012. **84**(9): p. 3973-3980.

64. Vijayakumar, M., et al., *Molecular structure and stability of dissolved lithium polysulfide species.* Physical Chemistry Chemical Physics, 2014. **16**(22): p. 10923-10932.

65. Hedman, B., et al., *Sulfur K-edge X-ray absorption studies using the 54-pole wiggler at SSRL in undulator mode.* Nuclear Instruments and Methods in Physics Research Section A: Accelerators, Spectrometers, Detectors and Associated Equipment, 1986. **246**(1-3): p. 797-800.

66. Alonso Mori, R., et al., *Electronic structure of sulfur studied by X-ray absorption and emission spectroscopy.* Analytical Chemistry, 2009. **81**(15): p. 6516-6525.

67. Patel, M.U.M., et al., *X-ray Absorption Near-Edge Structure and Nuclear Magnetic Resonance Study of the Lithium–Sulfur Battery and its Components.* ChemPhysChem, 2014. **15**(5): p. 894-904.

68. Janz, G., et al., *Raman studies of sulfur-containing anions in inorganic polysulfides. Potassium polysulfides.* Inorganic Chemistry, 1976. **15**(8): p. 1755-1759.

69. El Jaroudi, O., et al., *Raman spectroscopy study of the reaction between sodium sulfide or disulfide and sulfur: identity of the species formed in solid and liquid phases.* Inorganic chemistry, 1999. **38**(12): p. 2917-2923.

70. El Jaroudi, O., et al., *Polysulfide Anions II: Structure and Vibrational Spectra of the S42- and S52-Anions. Influence of the Cations on Bond Length, Valence, and Torsion Angle.* Inorganic chemistry, 2000. **39**(12): p. 2593-2603.

71. El Jaroudi, O., et al., *Polysulfide Anions. 1. Structure and Vibrational Spectra of the S22- and S32- Anions. Influence of the Cations on Bond Length and Angle.* Inorganic Chemistry, 1999. **38**(10): p. 2394-2401.

72. Wu, H.-L., L.A. Huff, and A.A. Gewirth, *In situ Raman spectroscopy of sulfur speciation in lithium–sulfur batteries.* ACS applied materials & interfaces, 2015. **7**(3): p. 1709-1719.

73. Hagen, M., et al., *In-situ Raman investigation of polysulfide formation in Li-S cells.* Journal of The Electrochemical Society, 2013. **160**(8): p. A1205-A1214.